

Samotherium Major, 1888 (Giraffidae) skulls
from the late Miocene Maragheh fauna (Iran)
and the validity of *Alcicephalus*
Rodler & Weithofer, 1890

Elnaz PARIZAD, Majid MIRZAI ATAABADI,
Marjan MASHKOUR & Dimitris S. KOSTOPOULOS



DIRECTEURS DE LA PUBLICATION / *PUBLICATION DIRECTORS* :
Bruno David, Président du Muséum national d'Histoire naturelle
Étienne Ghys, Secrétaire perpétuel de l'Académie des sciences

RÉDACTEURS EN CHEF / *EDITORS-IN-CHIEF* : Michel Laurin (CNRS), Philippe Taquet (Académie des sciences)

ASSISTANTE DE RÉDACTION / *ASSISTANT EDITOR* : Adeline Lopes (Académie des sciences; cr-palevol@academie-sciences.fr)

MISE EN PAGE / *PAGE LAYOUT* : Audrina Neveu (Muséum national d'Histoire naturelle; audrina.neveu@mnhn.fr)

RÉDACTEURS ASSOCIÉS / *ASSOCIATE EDITORS* (*, *took charge of the editorial process of the article/a pris en charge le suivi éditorial de l'article*) :

Micropaléontologie/*Micropalaeontology*

Maria Rose Petrizzo (Università di Milano, Milano)

Paléobotanique/*Palaeobotany*

Cyrille Prestianni (Royal Belgian Institute of Natural Sciences, Brussels)

Métazoaires/*Metazoa*

Annalisa Ferretti (Università di Modena e Reggio Emilia, Modena)

Paléoichthyologie/*Palaeoichthyology*

Philippe Janvier (Muséum national d'Histoire naturelle, Académie des sciences, Paris)

Amniotes du Mésozoïque/*Mesozoic amniotes*

Hans-Dieter Sues (Smithsonian National Museum of Natural History, Washington)

Tortues/*Turtles*

Juliana Sterli (CONICET, Museo Paleontológico Egidio Feruglio, Trelew)

Lépidosauromorphes/*Lepidosauromorphs*

Hussam Zaher (Universidade de São Paulo)

Oiseaux/*Birds*

Éric Buffetaut (CNRS, École Normale Supérieure, Paris)

Paléomammalogie (petits mammifères)/*Palaeomammalogy (small mammals)*

Robert Asher (Cambridge University, Cambridge)

Paléomammalogie (mammifères de moyenne et grande taille)/*Palaeomammalogy (large and mid-sized mammals)*

Lorenzo Rook* (Università degli Studi di Firenze, Firenze)

Paléoanthropologie/*Palaeoanthropology*

Roberto Macchiarelli (Université de Poitiers, Poitiers)

Archéologie préhistorique/*Prehistoric archaeology*

Marcel Otte (Université de Liège, Liège)

COUVERTURE / *COVER* :

Made from the Figures of the article.

Comptes Rendus Palevol est indexé dans / *Comptes Rendus Palevol is indexed by*:

- Cambridge Scientific Abstracts
- Current Contents® Physical
- Chemical, and Earth Sciences®
- ISI Alerting Services®
- Geoabstracts, Geobase, Georef, Inspec, Pascal
- Science Citation Index®, Science Citation Index Expanded®
- Scopus®.

Les articles ainsi que les nouveautés nomenclaturales publiés dans *Comptes Rendus Palevol* sont référencés par /
Articles and nomenclatural novelties published in Comptes Rendus Palevol are registered on:

- ZooBank® (<http://zoobank.org>)

Comptes Rendus Palevol est une revue en flux continu publiée par les Publications scientifiques du Muséum, Paris et l'Académie des sciences, Paris
Comptes Rendus Palevol is a fast track journal published by the Museum Science Press, Paris and the Académie des sciences, Paris

Les Publications scientifiques du Muséum publient aussi / *The Museum Science Press also publish*:

Adansonia, Geodiversitas, Zoosystema, Anthropolzoologica, European Journal of Taxonomy, Naturae, Cryptogamie sous-sections *Algologie, Bryologie, Mycologie*.

L'Académie des sciences publie aussi / *The Académie des sciences also publishes*:

Comptes Rendus Mathématique, Comptes Rendus Physique, Comptes Rendus Mécanique, Comptes Rendus Chimie, Comptes Rendus Géoscience, Comptes Rendus Biologies.

Diffusion – Publications scientifiques Muséum national d'Histoire naturelle

CP 41 – 57 rue Cuvier F-75231 Paris cedex 05 (France)

Tél. : 33 (0)1 40 79 48 05 / Fax : 33 (0)1 40 79 38 40

diff.pub@mnhn.fr / <http://sciencepress.mnhn.fr>

Académie des sciences, Institut de France, 23 quai de Conti, 75006 Paris.

© Publications scientifiques du Muséum national d'Histoire naturelle / © Académie des sciences, Paris, 2020
ISSN (imprimé / *print*) : 1631-0683/ ISSN (électronique / *electronic*) : 1777-571X

***Samotherium* Major, 1888 (Giraffidae) skulls from the late Miocene Maragheh fauna (Iran) and the validity of *Alcicephalus* Rodler & Weithofer, 1890**

Elnaz PARIZAD

School of Geology, College of Science, University of Tehran, Tehran (Iran)
parizad.elnaz@ut.ac.ir

Majid MIRZAIIE ATAABADI

Department of Geology, Faculty of Sciences, University of Zanjan, Zanjan (Iran)
majid.mirzaie@znu.ac.ir (corresponding author)

Marjan MASHKOUR

School of Geology, College of Science, University of Tehran, Tehran (Iran)
mashkour.marjan@ut.ac.ir

Dimitris S. KOSTOPOULOS

Laboratory of Geology and Palaeontology, School of Geology,
Aristotle University of Thessaloniki, Thessaloniki (Greece)
dkostop@geo.auth.gr

Submitted on 30 July 2019 | Accepted on 29 November 2019 | Published on 1 December 2020

[urn:lsid:zoobank.org:pub:D974D6AD-8792-4213-B573-116DE4117767](https://doi.org/10.5852/cr-palevol2020v19a9)

Parizad E., Mirzaie Ataabadi M., Mashkour M. & Kostopoulos D. S. 2020. — *Samotherium* Major, 1888 (Giraffidae) skulls from the late Miocene Maragheh fauna (Iran) and the validity of *Alcicephalus* Rodler & Weithofer, 1890. *Comptes Rendus Palevol* 19 (9): 153-172. <https://doi.org/10.5852/cr-palevol2020v19a9>

ABSTRACT

Samotherium Major, 1888 (Giraffidae) is recorded from several late Miocene localities, primarily in the Balkans, the northern Black Sea region, Anatolia, central Asia and China. The first complete cranial material, with several mandibular rami, and postcranials of *Samotherium* are described here from the Middle Maragheh sequence in northwest Iran. The Maragheh taxon appears metrically and morphologically similar to the smaller *Samotherium* taxon from the Samos Island (Greece) referred to as *S. boissieri* Major, 1888, type species of the genus. These new data trigger further discussion about the Iranian *Samotherium* record, including *Alcicephalus* Rodler & Weithofer, 1890, which was recently resurrected as a valid genus in the Maragheh fauna. Our analysis of the material referred to this genus indicates that *Samotherium* is the most likely attribution for the Maragheh *A. neumayri* Rodler & Weithofer, 1890. Differences between *S. boissieri* and *S. neumayri* are more pronounced in postcranial elements than in cranial and dental ones and need further investigation.

KEY WORDS

Samotherium,
Alcicephalus,
Paleotraginae,
Turolian,
Maragheh.

RÉSUMÉ

Crânes de Samotherium Major, 1888 (Giraffidae) de la faune du Miocène supérieur Maragha (Iran) et la validité d'Alcicephalus Rodler & Weithofer, 1890.

Samotherium Major, 1888 (Giraffidae) a été répertorié dans plusieurs localités du Miocène supérieur, principalement dans les Balkans, dans la région septentrionale de la mer Noire, en Anatolie, en Asie centrale et en Chine. Les premiers crânes complets ainsi que des mandibules de *Samotherium*, sont décrits ici à partir des horizons du Maragha moyen, dans le Nord-Ouest de l'Iran. Le taxon de Maragha

MOTS CLÉS
Samotherium,
Alcicephalus,
 Paleotraginae,
 Turolian,
 Maragha.

est métriquement et morphologiquement similaire au taxon plus petit de *Samotherium* de l'île de Samos (Grèce), appelé *S. boissieri* Major, 1888, espèce type du genre. Ces nouvelles données provoquent des discussions sur l'assemblage de *Samotherium* iranien, y compris *Alcicephalus* Rodler & Weithofer, 1890 récemment ressuscité comme genre valide dans la faune de Maragha. Nos analyses du matériel rapporté à ce genre indiquent que *Samotherium* est l'attribution la plus probable pour *A. neumayri* Rodler & Weithofer, 1890 de Maragha. Les différences entre *S. boissieri* et *S. neumayri* sont plus prononcées dans les éléments post-crâniens que dans les éléments crâniens et dentaires et nécessitent un examen plus approfondi.

INTRODUCTION

Eurasian late Miocene mammal communities (also known as the Pikermian faunas), distributed from Southern Europe and Balkans to Afghanistan and likely China, are characterized by a great variety of herbivore taxa, especially equids, rhinos, bovids and giraffids. Giraffidae themselves may be represented by up to five genera and species (e.g. *Palaeotragus* Gaudry, 1861, *Samotherium* Major, 1888, *Bohlinia* Matthew, 1929, *Helladotherium* Gaudry, 1860) in the same local/regional faunal context (Bernor 1984; Bohlin 1926; Bonis *et al.* 1992; Eronen *et al.* 2009; Kaya *et al.* 2018; Kostopoulos 2009a; Mirzaie Ataabadi 2010; Solounias *et al.* 1999, 2010), a diversity that the family never reached before or after this period.

Among late Miocene giraffids, *Samotherium* stands as one of the most common and widespread genera. It is known from the Turolian of Greece, Turkey, Iraq and Iran (Geraads 1978; Kostopoulos & Saraç 2005; Koufos 2013; Solounias & Danowitz 2016; Thomas *et al.* 1980), but also the northern Black Sea region (Vangengeim & Tesakov 2013), central Asia (Davyatkin 1981; Dmitrieva & Nesmejanov 1982; Kordikova 1998; Sotnikova *et al.* 1997; Tleuberdina 1988), China (Deng *et al.* 2013; Hou *et al.* 2019; Wang *et al.* 2013; Zhang *et al.* 2013) and possibly southern Italy (Marra *et al.* 2011) and Africa (Haile-Selassie 2009).

Samotherium was introduced by Forsyth-Major (1888) based on material from Samos Island, Greece, with *S. boissieri* Major, 1888 as the type species by monotypy. Much later, Geraads (1994) designated a skull from Samos in the collections of the Natural History Museum in London (NHML M4215) as the lectotype of the species. Bohlin (1926) described another larger form from Samos as *S. boissieri* var. *major* and Senyürek (1954) raised it to the species level. Geraads (1994) provided arguments for the distinction of the two species and designated a lectotype from Samos in the Natural History Museum at Basel (NHB Sa29) for *S. major*.

More than ten species are currently ascribed to *Samotherium* (e.g. Godina 2002 and references therein). However, most of them are poorly known and might be potential synonyms (i.e., Erdbrink 1977; Gentry *et al.* 1999; Kostopoulos 2009b) and thus an overall revision is essential.

Rodler & Weithofer (1890), obviously without being aware of the previous work of Forsyth-Major (1888), introduced *Alcicephalus* Rodler & Weithofer, 1890 for the two palaeotragine

giraffids recorded at Maragheh, northwest Iran; *A. neumayri* Rodler & Weithofer, 1890 later became the type species by “position precedence” (International Code Zoological Nomenclature, Article 69A.10). Mecquenem (1924-1925), in the first comprehensive work on the Maragheh mammal fauna, assigned several tooththrows and postcranials to the same species. Soon after, Bohlin (1926), in an in-depth study of the family Giraffidae, suggested that *Alcicephalus* is a junior synonym of *Samotherium*, a taxonomic decision followed by most later scholars until Hou *et al.* (2014), who recently re-introduced it as a valid genus.

Giraffids are important components in the late Miocene Maragheh fauna and among the first material recorded from this site (Bohlin 1926; Erdbrink 1976a, b, 1977, 1978; Grewingk 1881; Kittl 1885; Parizad *et al.* 2019). Evidence about *Samotherium* is however limited. Gunther (1896) first reported *S. boissieri* from Maragheh. Erdbrink (1976b, 1978) also referred to *Samotherium* material from Maragheh, including *S. boissieri*, but by proposing several subspecies presented a complex view of this taxon. Interestingly, *Samotherium* was absent or hardly represented in recent comprehensive works about Maragheh (Bernor 1986; Mirzaie Ataabadi *et al.* 2013). Recently, *Samotherium* material from old Maragheh collections has been mainly referred to *S. neumayri* (i.e., Bohlin 1926; Geraads 2017; Kostopoulos 2009b, among others), but cranial material referred to this species (see Fig. 4) is represented only by the holotype (maxilla and orbit) partial skull and a partial braincase (Bohlin 1926; Mecquenem 1924-1925; Rodler & Weithofer 1890). In the most recent revision of the Maragheh giraffids, Solounias & Danowitz (2016) recognized seven taxa, including *Alcicephalus* and *Samotherium*.

Here we report the recently excavated first complete skulls of *Samotherium* from Maragheh and re-discuss the Iranian record of the genus and its spatial and temporal range. We also argue for the validity of *Alcicephalus*.

GEOLOGICAL SETTING

The Maragheh bone beds are located in the East Azarbaijan Province, northwest Iran at the foothills of the Sahand Volcano (Fig. 1). Maragheh and its adjacent areas in the Azarbaijan region are characterized by repeated events of Cenozoic volcanic activity. The late Miocene in the Maragheh basin

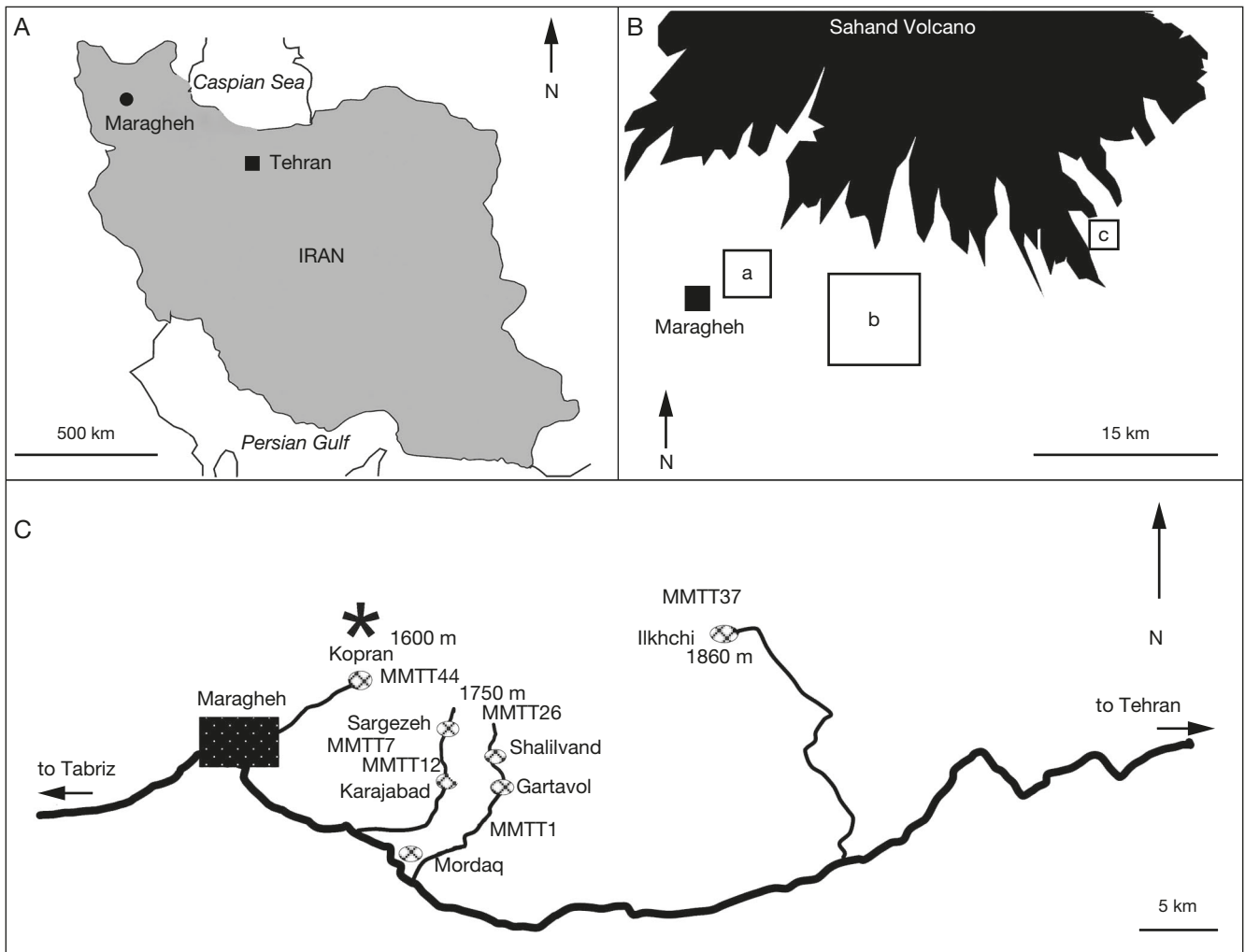


FIG. 1. — Location map of the study area and fossil sites in Maragheh area: **A**, position of Maragheh in northwest Iran; **B**, location of main Maragheh fossil zones (a, mainly Lower Maragheh sites; b, mainly Middle Maragheh sites; c, mainly Upper Maragheh sites) at the foothills of Mt Sahand (black silhouette); **C**, major fossil-bearing localities (UCR-MMTT sites) and their elevations in Maragheh, and the location of *Samotherium* Major, 1888 site (Ruhanioun locality) of this study (large asterisk).

includes a thick sequence of volcanoclastic continental beds known as the Maragheh Formation (Fm.). These beds seem to be deposited on the red terrestrial sediments, which formed after regression of the last seaways from this area in the early Neogene (Mirzaie Ataabadi *et al.* 2013).

The Maragheh Fm. is a 300-m-thick sequence, and the fossil-bearing strata are confined to its lower 150 m interval (Campbell *et al.* 1980; Kamei *et al.* 1977). The fossils have localized concentrations within this sequence (Bernor 1986) and they are oriented by paleo-currents (Mirzaie Ataabadi *et al.* 2013). Fluvial channel fills and floodplain depositional environments formed the fossil-bearing intervals. They include massive silty sand and sandy silt beds, commonly exhibiting paleosol formation. A few intercalations of laminated silts and small pond deposits are subordinate components of these sequences (Sakai *et al.* 2016).

The Maragheh Fm. consists of three litho/biostratigraphic intervals (Campbell *et al.* 1980); the Lower, Middle and Upper Maragheh. Boundaries of these three intervals were later refined by Bernor (1986) based on their distance from

the Loose Chippings marker layer. Thus, the Lower Maragheh is the interval ranging from –150 to –52 m from this marker bed. A few fossil sites occur at this interval. The intervals from –52 to –20 m from the Loose Chippings mark the Middle Maragheh. This is the most important unit, with the bulk of fossil material. The main fossiliferous areas in this unit are located between the villages of Mordagh and Karaj Abad (Fig. 1C). The Middle Maragheh was sampled by most of the research groups of the 19th and 20th centuries. An interval from –20 to +7 m from the Loose Chippings marker bed defines the Upper Maragheh.

The current elevation of the Maragheh fossil sites can be used further to distinguish these intervals. Localities with the lowest elevations (around 1500 m) belong to the Lower Maragheh and those with the highest altitude (more than 1800 m) belong to the Upper Maragheh. This is based on the slight dip of the strata of the Basal Tuff Fm., and consequently the Maragheh Fm., from east to west, which caused the accumulation of sediments earlier and at lower elevations in the western parts (Bernor 1986; Mirzaie Ataabadi *et al.* 2013).

TABLE 1. — Measurements (in mm) of *Samotherium cf. boissieri* Major, 1888 skulls from the Maragheh Formation, NW Iran. Bold numbers refer to measurements; (?) indicates uncertainty. Measurements: **1**, P2 to the anterior border of foramen magnum; **2**, P2 to the posterior margin of the orbit; **3**, P2 to the middle of the distance between the bases of the ossicones; **4**, P2 to the anterior border of choane; **5**, height from the alveolar level to the upper margin of the orbit; **6**, maximal breadth at the zygomatic arches; **7**, breadth behind the orbits; **8**, palatal breadth between the anterior end of P2; **9**, palatal breadth between the posterior end of M3; **10**, height of the occipital; **11**, length of the orbit; **12**, breadth of the orbit; **13**, length P2-M3; **14**, length P2-P4; **15**, length M1-M3; **16**, length of P2; **17**, width of P2; **18**, length of P3; **19**, width of P3; **20**, length of P4; **21**, width of P4; **22**, length of M1; **23**, width of M1; **24**, length of M2; **25**, width of M2; **26**, length of M3; **27**, width of M3.

Specimen	1	2	3	4	5	6	7	8	9	10	11	12	13	14
M351	390	260	240?	164	109.2	198	230	87.7	124	106.2?	79	49.4	185	75.8
M350		244	260?	150	140.4		214	74.6	112.8		63	59.2	183	74.5
	15	16	17	18	19	20	21	22	23	24	25	26	27	
M351	115.5	21.8	15.2	24.2	20.4	24.6	23	37.1	33.5	42.9	29.1	36.3	22.8	
M350	107.9	21.1	21.9	24.9	28	23.5	28.9	27.7	32	37.8	39		35	

The richly fossiliferous intervals of the Middle Maragheh have elevations of around 1700-1800 m. Material studied in this work comes from the Middle Maragheh horizons. They were excavated in recent years by MMTT/DOE from the Ruhanioon locality (N37°25'04", E46°17'22") near the suburbs of the city of Maragheh (Figure1C). The elevation of this site is 1689 m.

The chronological range of the Maragheh fossil localities is 9 to 7.5 Ma (Bernor 1986). An interpolation method used by Mirzaie Ataabadi *et al.* (2013: table 25.2) estimate the age of fossil localities and intervals based on their distance from the absolute-dated Loose Chippings marker bed. Using this method, localities with an elevation of around 1700 m (about -70 m distance from the marker bed) have an estimated age of 8.3 Ma. This is in agreement with the recent magnetostratigraphic studies that provided an approximate age of 8.1-7.7 Ma for fossil levels at 1720 m elevation (Mirzaie Ataabadi *et al.* 2016; Salminen *et al.* 2016). Therefore, the Maragheh *Samotherium* material studied here has an estimated age of 8.0-8.3 Ma (MN11 equivalent). Among the American UCR-MMTT fossil sites excavated in the 1970's, those situated in the Ali Abad and Dare Gorg areas are chronologically close to the studied locations. These include MMTT 8, 23, 28, 36, and 42 (Mirzaie Ataabadi *et al.* 2013; Parizad *et al.* 2019).

MATERIAL AND METHODS

The two almost complete skulls (PRCI/M350-351), several mandibles (PRCI/M310-313) and some postcranials (PRCI/M312, 174, 294, 296-300) are stored in the Paleontological Research Center of Iran in Maragheh. Cranial measurements and descriptions follow Kostopoulos *et al.* (1996 and literature therein), and Kostopoulos (2009b). All the measurements are in millimeters. Dental and postcranial material are presented in the Supplementary Material.

ABBREVIATIONS

AMNH	American Museum of Natural History, New York;
BSPG	Bayerische Staatssammlung für Paläontologie und Geologie, Munich;
DOE	Department of Environment (environment protection organization of Iran);
HMV	Hezheng Paleozoological Museum, Gansu;

IVPP	Institute of Vertebrate Paleontology and Paleoanthropology, Beijing;
MMTT	Muze Melli Tarikh Tabaeie (i.e., National Museum of Natural History in Persian), Tehran;
MNHN	Muséum national d'Histoire naturelle, Paris;
NHB	Natural History Museum, Basel;
NHMUK	Natural History Museum, London;
NHMW	Naturhistorisches Museum, Wien;
PRCI	Paleontological Research Center of Iran;
UCR	University of California, Riverside;
MN	European Neogene land Mammal units;
M, m	Upper and lower molars;
P, p	Upper and lower premolars;
Mt	Metatarsal;
Mc	Metacarpal;
Ast	Astragalus.

SYSTEMATIC PALEONTOLOGY

Class MAMMALIA Linnaeus, 1758
Order ARTIODACTYLA Owen, 1848
Suborder RUMINANTIA Scopoli, 1777
Family GIRAFFIDAE Gray, 1821
Genus *Samotherium* Forsyth-Major, 1888
Type species *Samotherium boissieri* Forsyth-Major, 1888

Samotherium cf. boissieri
(Figs 2; 3; Table 1; Appendices 2; 3; 5)

REFERRED MATERIALS. — Two almost complete skulls (PRCI/M350-351), and four mandibles (PRCI/M310-313).

PROVISIONALLY ASCRIBED MATERIALS. — Two metapodials (PRCI/M174, 312) and six astragali (PRCI/M294, 296-300), from the Ruhanioon locality, Maragheh, Iran.

DESCRIPTION

Two hornless skulls (PRCI/M350-351) were discovered. The skull PRCI/M350 belongs to an older adult individual. The back of the brain case and the premaxillary part of the face are not preserved in this specimen (Fig. 2). The skull PRCI/M351 is from an adult individual. It preserves most of the skull except the premaxillary part (Fig. 3). Both skulls are a little compressed laterally, but they preserve most of their morphometrical features.

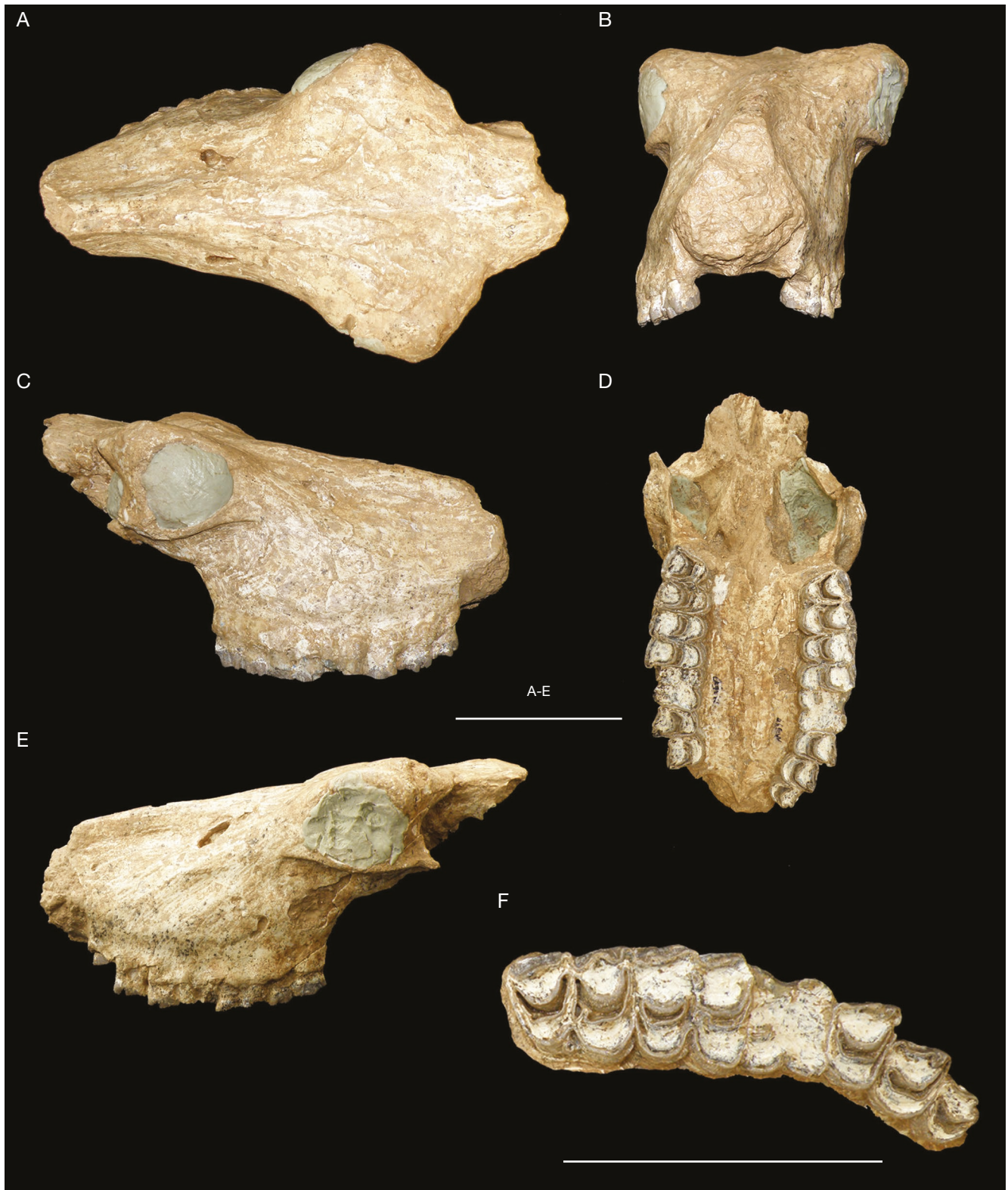


FIG. 2. — *Samotherium* cf. *boissieri* Major, 1888 skull PRCI/M350 from Ruhanioun locality, Maragheh, NW Iran: **A**, dorsal view; **B**, right lateral view; **C**, left lateral view; **D**, frontal view; **E**, ventral palatine view; **F**, enlarged occlusal view of the right tooth row. Scale bars: 10 cm.

The opisthocranium is especially short in relation to the face (Fig. 3A, C, E). The basicranial angle (i.e., the angle between the basicranial surface and the occlusal surface of the cheek teeth) is around 15°. The occipital condyles are strong and

point postero-ventrally (Fig. 3C-E). The basioccipital is short (Fig. 3F) and triangular, with much stronger posterior than anterior tuberosities. The paraoccipital processes are broken, but clearly placed in front of the condyles. The foramen magnum

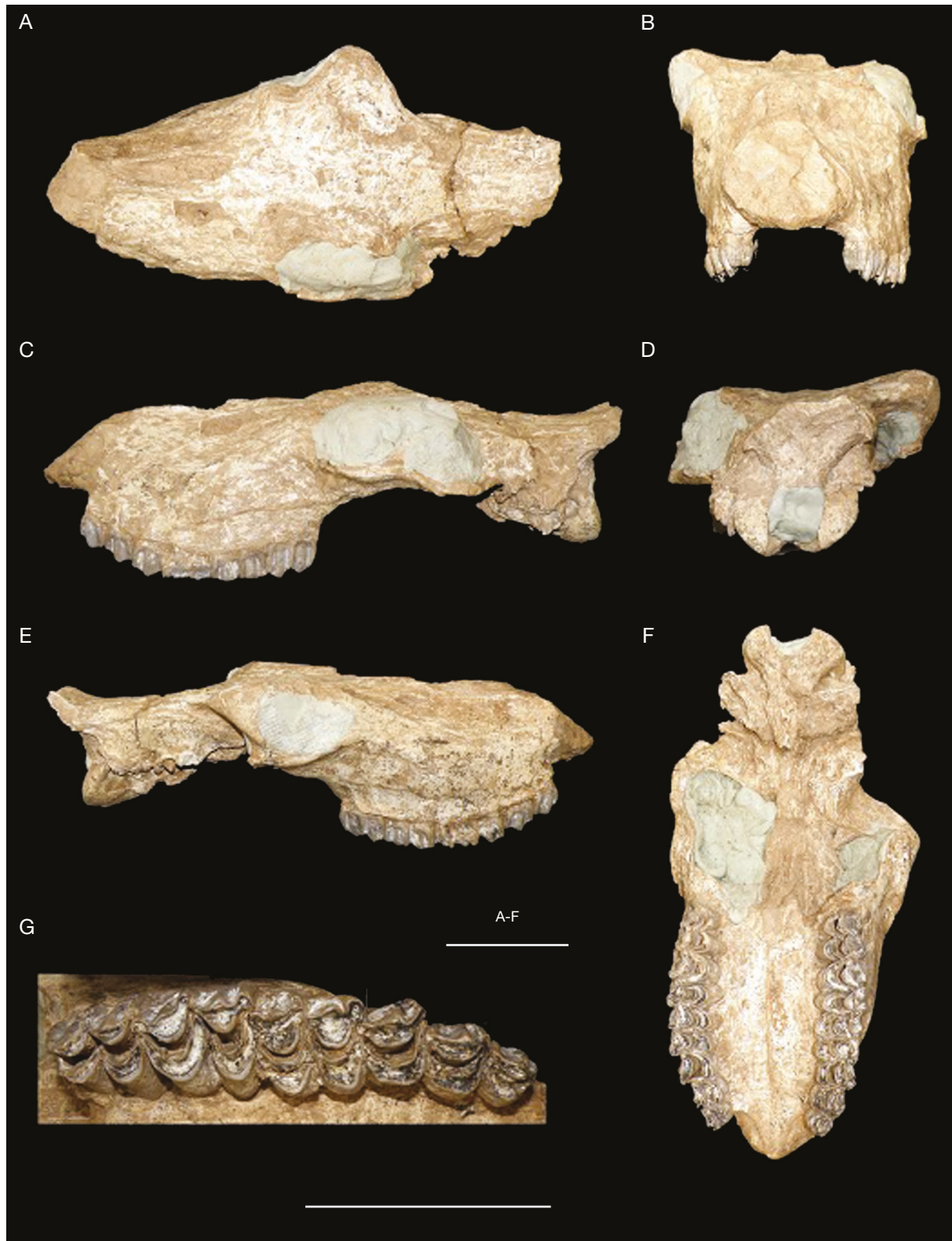


FIG. 3. — *Samotherium* cf. *boissieri* Major, 1888 skull PRCI/M351 from Ruhanioun locality, Maragheh, NW Iran: **A**, dorsal view; **B**, left lateral view; **C**, right lateral view; **D**, enlarged occlusal view of the right tooth row; **E**, frontal view; **F**, caudal view; **G**, palatine view. Scale bars: 10 cm.

is filled with paste but seems to be quadrangular. The occipital face looks rectangular with a characteristically fan-shaped occiput (Fig. 3D). The nuchal crest is strong, posteriorly projected and has a median notch (Fig. 3D). The braincase

roof is undulated in lateral aspect (Figs 2B; 3B) with a slightly convex rostral and a concave caudal part, exaggerated by the strong nuchal crest. Temporal crests are strong (Figs 2A; 3A); they slightly diverge rostrally and converge caudally.

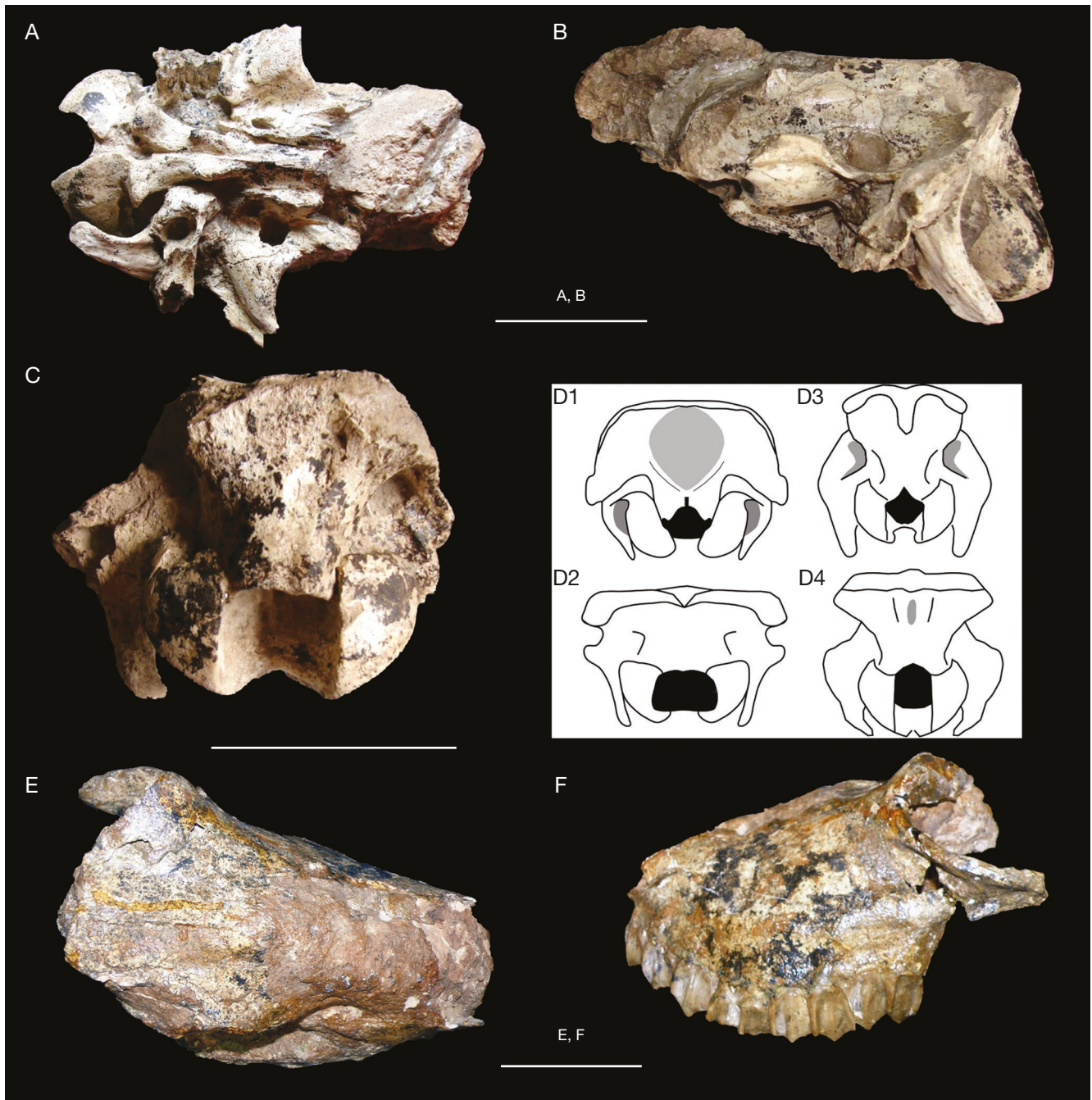


FIG. 4. — *Samotherium neumayri* (Rodler & Weithoffer, 1890) cranial specimens from Maragheh, NW Iran and comparison of occipital shapes. **A–C**, the braincase MNHN MAR651 in: **A**, ventral; **B**, left lateral; and **C**, caudal view. **D**, drawings depicting the two types of giraffid occipital shape discussed by Hou *et al.* (2014); **D1**, **D2**, the “broad occipital” type referred by Hou *et al.* (2014) to *Alcicephalus* Rodler & Weithofer, 1890; **D3**, **D4**, the “fan shaped” (or “hour-glass”) type of **D3** *Samotherium boissieri* Major, 1888 and **D4** *Palaeotragus coelophrys* (Rodler & Weithoffer, 1890) (adopted from Hou *et al.* (2014: fig. 1 based on Chinese crania). **E**, **F**, the holotype palate NHMW 2019/0018/0006 of *S. neumayri* in: **E**, dorsal; and **F**, left lateral view (courtesy of the NHMW and Ursula Göhlich). Scale bars: 10 cm.

The upper margin of the external auditory meatus is below the lower orbital level (Fig. 3C). The alveolar level is subparallel to the naso-parietal one (Figs 2; 3C, E). The zygomatic arches run parasagittally. The frontals are wide and slightly concave. Extended lachrymal sinuses form a small hump in the rostro-dorsal part of the orbit, at the level of the fronto-lachrymal suture (Figs 2; 3C, E). The nasals are elongated and thin. Their widened posterior part is placed above the M2-M3 level (Figs 2A; 3A). A small ethmoidal fissure is formed by the

nasal, lachrymal and maxillary bones. Its posterior margin is placed above M1-M2 (Fig. 3C, E). A triangular lachrymal depression, with an anterior limit above P3/P4, is defined by the nasals, and a blunt crest running obliquely from the fronto-lachrymal area (Figs 2; 3C, E). A slightly developed facial crest extends up to M1 (Figs 2; 3C, E). The infraorbital foramen opens above and slightly in front of P2 (Fig. 3C). The orbit is round and its upper half is above the nasal level (Figs 2; 3C, E) having an elevated “periscopic” position.

The anterior margin of the orbit is placed above the posterior lobe of M3 (Figs 2; 3C, E). The supraorbital process of the frontals is well developed and extended (Figs 2A; 3A). The thickness of the frontals is about 20 mm at the orbital region. The choanae are open, “V”-shaped, and extend rostrally to the middle of M3 and anterior to the lateral indentations of the palate (Fig. 3F).

The length of the upper toothrow ranges from 183 to 185 mm ($n = 2$) with a premolar/molar length ratio of 65.6–69.0 (Figs 2F; 3G). The p2–m3 length is 189–190 mm with a lower premolar/molar length ratio from 58 to 63 (mean = 60.5, $n = 4$). Detailed morphological descriptions of the upper dentition, mandibles and lower dentition (Appendix 2) are provided in the Supplementary Material (Appendix 1). Descriptions and measurements of the postcranials (Appendix 5) provisionally associated with the studied cranial material are also given in the Supplementary Material (Appendix 1).

COMPARISON

The cranial, dental and postcranial morphology and proportions of the studied material preclude ascription to Sivatheriinae: with much larger size, larger premolars compared to the molars, unmolarized p3, more massive metapodials; or Giraffinae: comparatively shorter braincase, domed nasals, more complex dental morphology, dolichopodial limbs; suggesting affiliations to Palaeotraginae (Hamilton 1978; Geraads 1986). The two studied skulls are determined as females because of the absence of ossicones and related bumps on the frontals. As seen in specimens from Greece, Turkey, Iran and China, “hornless” females are rather common within the subfamily Palaeotraginae, although occasional thin ossicones on females sometimes occur (Bohlin 1926; Kostopoulos 2009b).

Three palaeotragine genera are reported from Maragheh: *Palaeotragus*, *Samotherium* and *Alcicephalus* (Bohlin 1926; Mecquenem 1924–1925; Solounias & Danowitz 2016). The backward position of the orbit, the large toothrow and especially the large molars, the short upper premolar row compared to the molars, the strong paracone and metacone pillars, the weak metastyle, the non-constricted linguall protocone, the presence of a medial spur on the mesial flange of the hypocone on the upper molars, the undistinguished paracone and metacone on the upper premolars, the short diastema compared to the toothrow (p2–m3) length (length ratio well below 1), and the reduced talonid of the lower p3 and p4, differentiate the studied crania and mandibles from the similar-sized *Palaeotragus coelophrys* (Rodler & Weithofer, 1890) from Maragheh (Bohlin 1926; Geraads 1986, 1994; Hamilton 1978; Kostopoulos 2009b).

Alcicephalus versus *Samotherium*

Recent revisions have revived the debate over the validity of the genus *Alcicephalus*, originally introduced by Rodler & Weithofer (1890) for the large Maragheh samotheres. According to Hou *et al.* (2014), the occipital of *Alcicephalus* does not form a protruding backward shelf as in *Samotherium* and *Palaeotragus*, lying on the same flattened or slightly concave surface along with the mastoids. This morphology is mainly

observed on two Chinese crania from Gansu ascribed to *Alcicephalus* (NS 20 HMV 0948 and NS 8 HMV 0947; see Hou *et al.* 2014: fig. 1 and fig. 4D1, D2). However, Hou *et al.* (2014: 92) recognized a similar occipital pattern on a braincase from Maragheh, referred to the same taxon [specimen MNHN MAR651, Fig. 4A–C, originally described and illustrated by Mecquenem (1924–1925: pl. II, fig. 3) as *Camelopardalis attica* Gaudry & Lartet, 1856 and incorrectly listed as MNHN MAR681 by Hou *et al.* (2014) and Solounias & Danowitz (2016)]. Because MNHN MAR651 is widely accepted as conspecific with the holotype palate of *A. neumayri* [NHMW 2019/0018/0006, Fig. 4E, F, previously reported as NHMW A4903 and incorrectly listed as MNHNW A4960 by Solounias & Danowitz (2016)], Hou *et al.* (2014) suggested *Alcicephalus* is a distinct genus, admitting however the similarities with *Samotherium* in size and morphology. These specimens (MNHN MAR651 and NHMW 2019/0018/0006; Fig. 4) together with some isolated ossicones, dentitions, and postcranials from Maragheh (stored in NHMW, MNHN Paris, MMTT Iran, AMNH New York, and BSPG Munich) contributed to the hypodigm of *A. neumayri* in Solounias & Danowitz (2016), and allowed these authors to provide a composite reconstruction of its skull (*idem*: fig. 5). In distinction of *Samotherium*, *Alcicephalus* is also reported as having a notably small masseteric fossa, inward curved ossicones, low mandibular ramus, and short lamina and lack of a dorsal tubercle on the atlas (Hou *et al.* 2014; Solounias & Danowitz 2016).

In our view, the occipital of MNHN MAR651 clearly shows a protruding fan-shaped shelf placed on a more caudal level than the mastoids (Fig. 4C), similar to *Samotherium* and *Palaeotragus* (Fig. 4D3, D4) and in contrast to the Chinese crania (Fig. 4D1, D2) studied by Hou *et al.* (2014). The basicranial morphology of the specimen (Fig. 4A) is also completely compatible to that of *Samotherium* from Samos and China. Furthermore, we were not able to trace any significant difference in the degree of masseteric fossa development between the badly preserved NHMW 2019/0018/0006 (Fig. 4E, F) and most *Samotherium* crania from Samos or in the depth of the mandible (with the height of the mandible between p4–m1 nearly equal to the length of m3). The inward curvature of the ossicones does not seem to be a valid character for genus distinction, as for instance, ossicones of the closely related *Palaeotragus* may be quite variable depending on the species (Athanasio 2014; Bohlin 1926). Hence, cranial, mandibular and dental features of the Maragheh material are consistent with the characteristics of the genus *Samotherium* and not sufficient for the re-establishment of *Alcicephalus*. As a consequence the generic attribution of the Gansu crania studied by Hou *et al.* (2014) needs reconsideration.

Cranial comparisons among Samotherium boissieri, *S. neumayri* and *S. major*

Several scholars suggested synonymizing *S. neumayri* (Rodler & Weithofer, 1890) with *S. boissieri* Major, 1888 or *S. major* Bohlin, 1926 (Erdbrink 1978; Gentry *et al.* 1999). Although cranial and dental size and morphology of *S. neumayri* are

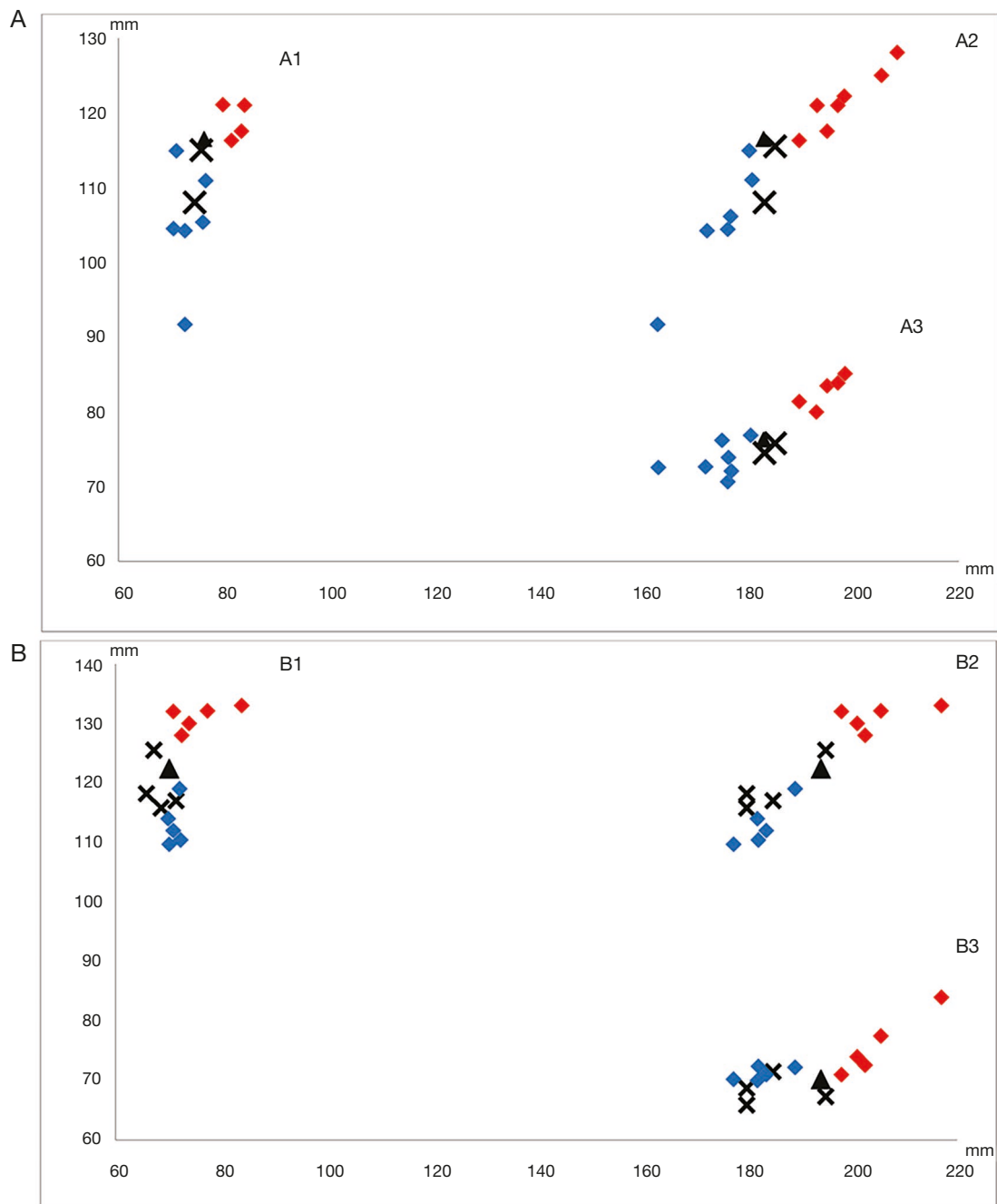


FIG. 5. — Scatter diagram, comparing the dental parameters of *Samotherium* cf. *boissieri* Major, 1888 (×) and *S. neumayri* (Rodler & Weithoffer, 1890) (▲) from Maragheh, Iran with *S. boissieri* (blue ♦) and *S. major* Bohlin, 1926 (red ♦) from Samos, Greece. Horizontal and vertical axis represent dental measurements in millimeters. Samos data after Kostopoulos (2009b). **A**, Upper dentition: **A1** (LP2-P4/LM1-M3); **A2** (LP2-M3/LM1-M3); **A3** (LP2-M3/LP2-P4). Maragheh specimens (PRCI/M350 - 351). **B**, Lower dentition: **B1** (Lp2-p4/Lm1-m3); **B2** (Lp2-m3/Lm1-m3); **B3** (Lp2-m3/Lp2-p4). Maragheh specimens (PRCI/M310 - 313).

quite similar to those of *S. boissieri* (Fig. 5A, B). Postcranials from Maragheh referred to *S. neumayri* appear proportionally intermediate between those of *S. boissieri* and *S. major* (Geraads 2017; Hou *et al.* 2014; Kostopoulos 2009b; Rios *et al.* 2017; Solounias & Danowitz 2016; Appendix 6) and therefore are in favor of its distinction as a separate species. Although generic disparity is suggested for *S. boissieri* and *S. major* (Solounias 2007), data support the presence of two distinct species (Geraads 1994; Kostopoulos 2009b; Rios *et al.* 2017). *Samotherium boissieri*, *S. neumayri* and *S. major*

share the large size and the long-pointed frontal appendages (unknown in *S. neumayri*), the reduction of the posterior lobe of p4, the relatively elongate p2, the short premolar row, and the large and rather massive limbs (Geraads 1986; Hamilton 1978; Kostopoulos 2009b).

The elevated “periscopic” position of the orbit is more developed in *S. boissieri* than in *S. major*. It means that while half of the orbit is placed above the upper surface of the nasal level in *S. boissieri*, only 1/3 of the orbit exceeds this level in *S. major*. In addition, the orbit is more posteriorly placed

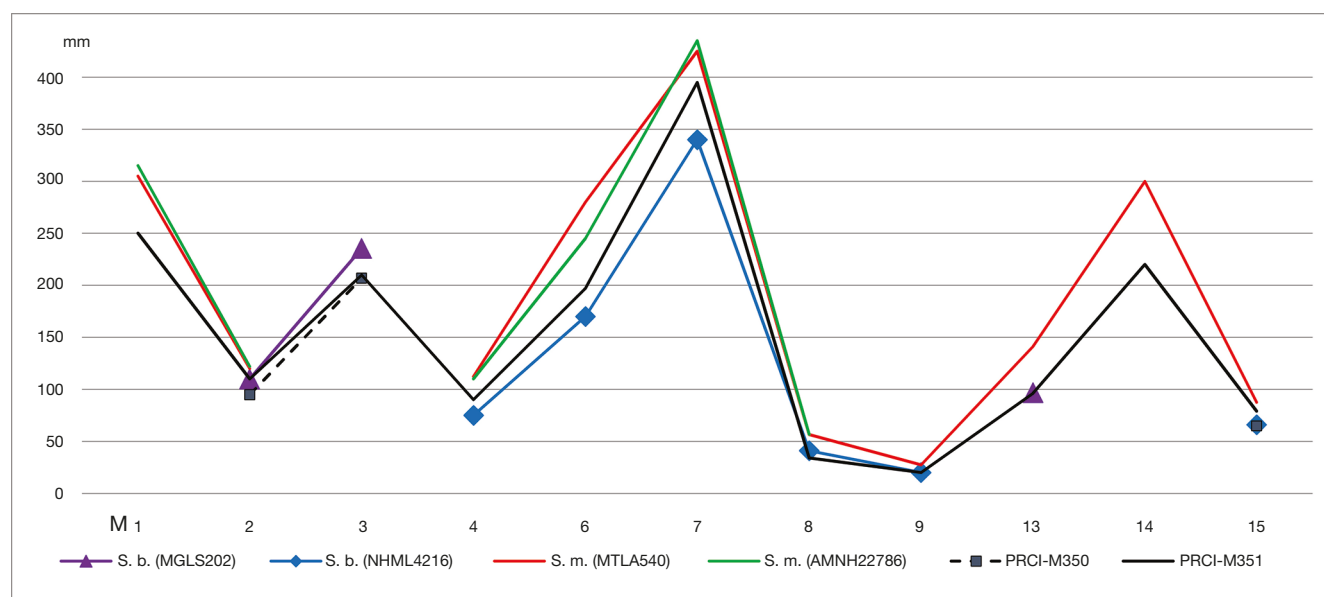


Fig. 6. — Line diagram comparing the skulls of *Samotherium cf. boissieri* Major, 1888 from Maragheh, Iran (PRCI/M350 – 351), with *S. boissieri* (S. b.) and *S. major* Bohlin, 1926 (S. m.) from Samos, Greece. Horizontal axis represents skull measurements (M1–15 as described below) and the vertical axis is the corresponding values in millimeters. Samos data and measurements after Kostopoulos (2009b). Numbers: **1**, length from the midpoint between the anterior margin of the orbits to the nuchal crest; **2**, width of the braincase; **3**, maximum width at the posterodorsal corner of the orbits; **4**, bi-condyle width; **6**, length from basion to the back of M3; **7**, length from basion to the front of P2; **8**, width at the posterior tuberosities of the basioccipital; **9**, width at the anterior tuberosities of the basioccipital; **13**, max width of the nuchal crest; **14**, length from basion to the anterior margin of the choanae; **15**, horizontal diameter of the orbit.

in *S. major* than in *S. boissieri* (Kostopoulos 2009b). In all these respects the new samotheres material from Maragheh is closer to *S. boissieri* than to *S. major*. Comparison with *S. neumayri* is restricted to the holotype palate NHMW 2019/0018/0006, which is seriously damaged at the orbito-nasal area (pers. obs. and Rodler & Weithofer 1890: taf. II, fig. 2). However, the orbit appears to have a quite advanced elevated “periscopic” position and its anterior edge is above the M3 (Fig. 4E, F), similarly with the studied crania. The lachrymal depression in *S. major* is much wider and longer than in *S. boissieri* and the new Maragheh crania. The ethmoidal fissure is defined by the same bone elements in both taxa, but it is much smaller in *S. major*. The posterior margin of this fissure is above the M3 in this species, but above M1–M2 in *S. boissieri* and in the new Maragheh crania. Unfortunately, these features are not securely recognizable in the holotype of *S. neumayri*. In *S. boissieri* and the new Maragheh specimens the choanae are open “V”-shaped, reaching the middle of M3. Whilst in *S. major* it is U-shaped, invading farther anteriorly (until the anterior border of M3). In *S. neumayri* the choanae open slightly behind the lateral indentations, in contrast to the studied material (MAR 350–351; Figs. 2D; 3F), where the lateral indentations are retracted at the distal edge of M3 and the choanae open anterior to them, reaching the middle of M3.

The paroccipital processes in *S. major* have a more vertical position than in *S. boissieri* and *S. neumayri*. They reach below the condyle level, whereas the basioccipital is also longer in *S. major* but with a similar structure. In opisthocranial features the studied Maragheh crania more resemble *S. boissieri* and *S. neumayri* than *S. major*. Metrical skull characters of the new Maragheh specimens are generally smaller than those of *S. major* and closer to *S. boissieri* and *S. neumayri*

(Figs 5; 6). The general shape and outline of the mandible is similar between *S. major* and *S. boissieri*. However, the ventral profile of the horizontal ramus is more open “S” shaped in *S. boissieri* and in the Maragheh specimens studied here than in *S. major*. No complete mandible of *S. neumayri* is known for comparison.

Dental comparisons of *Samotherium boissieri*, *S. neumayri* and *S. major*

The tooth morphology of *S. boissieri* is generally similar to that of *S. major* and *S. neumayri* and a distinction is difficult, given that great morphological variability observed in samotheres (e.g. Bohlin 1926; Kostopoulos 2009b). The upper and lower dental metrical features (length of premolar to molar row, and length of tooth row to length of premolar and molar row) of the studied Maragheh samotheres are smaller than those of *S. major* and within the range of *S. boissieri*, but also close to the known values for *S. neumayri* (Fig. 5). An investigation of dental differences between the similar-sized *S. boissieri* from Samos and *S. neumayri* from old Maragheh collections (MNHN, NHMW, MMTT) is attempted. The comparison focuses on the lower premolar morphology considered by some authors to be more diagnostic (e.g. Geraads 1978, 1994; Hamilton 1978). It should be noted, however, that the sample is just indicative ($n = 8$ –12) and that old Maragheh collections do not always have precise stratigraphic provenience, meaning that there is a risk that the sample considered here as representing *S. neumayri* may contain specimens of different dating (and possibly species taxonomy).

Similar to *S. boissieri* and different from *S. neumayri* (but observations based only on the MNHN MAR 528 mandible and an uncatalogued p4–m3 series in NHMW), the studied

lower molars have a weakly expressed parastylid and more triangular-shaped hypoconid (instead of strong parastylid and highly convex and wide hypoconid in *S. neumayri*). In two of the four available mandibles bearing the second premolar (Appendix 4A-B), the p2 length represents 80.5–84.5% of the p3 length. In *S. boissieri* from Samos, the p2 to p3 length ratio ranges from 75.2–85.5 (n = 5), whereas in *S. neumayri* the p2 appears relatively shorter (70.7–72.0%; n = 2). In all studied samples the p3 length represents about 80–90% of the p4 length, whereas the talonid to trigonid length ratio of p4 ranges from 30 to 48% (n = 10), though a p4 in NHMW shows an even shorter talonid (26%). There are three main morphotypes of p3: those in which the metaconid fuses earlier with the entoconid than with the paraconid (type I), those in which the metaconid fuses earlier with the paraconid than with the entoconid (type II), and those with a fully molarized lingual wall even from unworn stage (type III). The last type appears in every one of the studied samples and usually these p3s look like perfect copies of the corresponding p4s. Type I of p3 rather characterizes *S. boissieri* from Samos and it also occurs in two out of the three studied p3s (Appendix 4). Type II appears in one of the two known p3s attributed to *S. neumayri* (MNHN MAR528), and the other (uncatalogued specimen in NHMW) represents type III.

All three p4s from the Ruhanioon locality show a short hypoconid-entostylid complex associated with a short and almost mesio-distally arranged entoconid, sometimes leaving the posterior valley open distally (type 1). Four of the five p4s of *S. neumayri* known to us show an elongated entoconid and a long continuous hypoconid-entostylid complex, closing the posterior valley (type 2). The fifth p4 follows type 1. In *S. boissieri* from Samos there are variants of both morphotypes (Kostopoulos 2009b: fig. 8). All three p4s from the Ruhanioon locality show a strong parastylid resembling *S. neumayri* more than *S. boissieri*.

DISCUSSION

In agreement with Bohlin (1926), our study reveals that cranial and dental features of the Maragheh samotheres are clearly within the range of distinctive characters of the genus *Samotherium* and thus the revival of the genus *Alcicelaphus* seems unnecessary. In contrast to Solounias & Danowitz (2016) and Xafis *et al.* (2019), we suggest that particular postcranial features and proportions of the Maragheh samotheres are applicable only at the species level.

The cranial material from Maragheh described herein is morphometrically compatible with both *S. boissieri* and *S. neumayri*. The differences of these species are more pronounced in postcranial elements than in cranial and dental ones, and need further investigation. The only cranial difference we detected between the studied crania and *S. neumayri* concerns the deepness and overall outline of the choanae. However, it is clearly not enough for secure conclusions. Dentally, the studied samotheres material better approaches *S. boissieri* than *S. neumayri*, though distinction based on dental features is not

always straightforward. The studied postcranials (if indeed of the same taxon or partly at least; see Comparison in Appendices), suggest that the studied crania may be associated with relatively small skeletal elements within the range of variation of *S. boissieri* from Samos and less robust than those ascribed to *S. neumayri* (Appendix 6). Hence, taking into account all the information available, we refer the *Samotherium* from the Ruhanioon locality to *Samotherium* cf. *boissieri*.

Apart from *Samotherium neumayri* and *Palaeotragus coelophrys*, Solounias & Danowitz (2016) recognized both *S. boissieri* and *S. major* at Maragheh. The occurrence of *S. major* in Maragheh is based on two astragali and a metatarsal (Solounias & Danowitz 2016: 498). Nevertheless, two of the three mentioned specimens (the astragalus MNHN MAR838 and the metatarsal MNHN MAR571) are in our opinion indistinguishable from other *S. neumayri* postcranials in the MNHN Paris collection (Appendix 6A, C). Material attributed by the same authors to *S. boissieri* is in our opinion questionable because it may represent (or be mixed with) *P. coelophrys* (e.g. Geraads 2017: fig. 3). Xafis *et al.* (2019) also record *S. boissieri* and *S. neumayri* together in Kavakdere, central Anatolia. Nevertheless, the two specimens (an astragalus and a calcaneum) ascribed by these authors to *S. boissieri* are metrically indistinguishable and morphologically closer to a large *Palaeotragus* (as shown by the concave plantar edge of the calcaneal body, the protruding and pointed tuber calcis, the absence of a notch between the proximal edge of the articular surface for the cuvonavicular and the distal edge of the plantar surface of the calcaneum, the straight lateral margin of the astragalus without a notch, the strong medio-plantar projection of the medial trochlear ridge of the astragalus, the very weak distal intracarpal fossa, and the less oblique medial ridge). Hence, the apparent coexistence of *S. neumayri* with either *S. boissieri* or *S. major* is debatable.

The new data provided in this study together with recent data by Hou *et al.* (2019) and previous data from Greece and Turkey (Geraads 1994; Kostopoulos 2009b and references therein) suggest that *S. boissieri* was a widespread giraffid taxon mainly distributed from western Anatolia to China, and possibly to southern Italy and Africa. The Greek, Turkish and Iranian records indicate an early Turolian equivalent age for this taxon (Geraads 1994; Kostopoulos 2009b; Mirzaie Ataabadi *et al.* 2013). *S. boissieri* from the Linxia Basin in China (Hou *et al.* 2019) comes from the Liushu Formation that spans most of the Vallesian and the lower half of the Turolian (Deng *et al.* 2013; Qiu *et al.* 2013). Although a better age estimate is not currently available (Zhang Zhaoqun pers. com. 2019), rough contemporaneity between *S. boissieri* from China and Central-West Asia cannot be excluded. The mid-late Turolian record of *S. boissieri* from Taraklia (Vangenheim & Tesakov 2013) is debatable. Godina (2002) refers the atlas and axis of the Taraklia samotheres to a new taxon, *S. borissiakii*, but according to her remarks the specimens are similar in size to the larger samotheres from Samos.

The timing of *Samotherium*'s emergence and its origin are still unknown, although there is consensus among authors about the closest relationships with *Palaeotragus* (Bohlin 1926;

Geraads 1986; Solounias 2007). Deng *et al.* (2013) record *Samotherium* sp. from the late Vallesian equivalent Dashengou fauna in Linxia Basin, whereas Vangenheim & Tesakov (2013) report *Samotherium* sp. from the late MN9- MN10 faunas of Berislav, Staraya Kubanka and Novoukrainka in the north shores of the Black Sea. It is therefore possible that *Samotherium* arises during Vallesian from the *Palaeotragus* stock. But, since the monophyly of the genus is rather unlikely (e.g. Geraads 1986; Rios *et al.* 2017), its appearance may have taken place in parallel in eastern and western Asia. With these doubts, it is difficult to see if the rather simultaneous appearance of *S. boissieri* in Iran, China, and western Anatolia represents a single dispersal event, as it looks at first glance, even though the taxon originates from northeast Asia or northern Paratethys.

In each of these geographic sectors (North Black Sea, Iran, China, western Anatolia), *Samotherium* is represented in later times by larger species (*S. eminens*, *S. neumayri*, *S. sinense*, and *S. major* respectively) in an asynchronous sequence from early to late Turolian age. Although in Samos early and later *Samotherium* appear to represent a morphocline (Kostopoulos 2009b), it is not easy to identify this morphocline in other regions. The morphological similarities between the new *S. cf. boissieri* material described here and *S. neumayri*, decrease the taxonomic distance between these two species and may also be in favor of a second cline in Iran and surroundings. Nevertheless, the available data are still insufficient for safe conclusions. An alternative hypothesis would be that specimens at present attributed to *S. neumayri* (including Chinese samples) do not really represent a distinct species but an Asiatic variation inside the *S. boissieri*-*S. major* sequence. *Samotherium neumayri* from Kavakdere (Xafis *et al.* 2019) may favor this option.

Research on fossil giraffid paleodiet using several methods show a high dietary heterogeneity among the Turolian taxa. *Samotherium major* was likely a grazer, *Palaeotragus* spp., *S. neumayri* and *S. boissieri* were seasonal mixed feeders while *Bohlinia attica* and *Helladotherium duvernoyi* were browsers (Danowitz *et al.* 2016; Merceron *et al.* 2018; Solounias *et al.* 2000, 2010, 2013). These data suggest that grazing, mixed feeding, and browsing took place in the forest and woodland environments of the Eurasian late Miocene. The presence of *S. cf. boissieri* and *Bohlinia attica* (Parizad *et al.* 2019) in the Ruhanioun locality and the abundance of mixed feeding taxa among Maragheh giraffids suggest a significantly wooded environment of Maragheh, as suggested by previous studies (Bernor *et al.* 2014; Mirzaie Ataabadi *et al.* 2013; Yamada *et al.* 2016).

CONCLUSIONS

The first skulls of *Samotherium* attributed to *S. cf. boissieri* were reported from the Maragheh bone beds of northwest Iran. The skulls are hornless with a well-developed periscopic position of the orbits. The occiput is caudo-dorsally projected and fan-shaped. A well-defined lachrymal depression is present. This material significantly enriches what is known from

this genus in Maragheh and leads us to re-discuss its presence in the area, as well as the validity of *Alcicephalus*. Our study of Maragheh materials recently referred to *Alcicephalus* does not confirm this assignment and suggests that *Samotherium* is a better attribution for the Maragheh *Alcicephalus neumayri*.

The occurrence of *S. cf. boissieri* in Maragheh is chronologically similar to or slightly older than that of Samos (MN11) and roughly contemporaneous with *S. boissieri* from China. The available data allow us to suggest an early Turolian pan-Asian dispersal of *S. boissieri*, which likely represents the ancestral stock of several later Eurasian samotheres of larger body mass. However, further investigation is needed to proof the taxonomic validity of *S. neumayri* and to understand its meaning within the *S. boissieri* – *S. major*/*S. sinensis* sequence.

Acknowledgements

We thank MMTT/DOE for permission to access and study of the specimens. Zahra Orak (DOE, Tehran) and Gholamreza Zare (DOE, Maragheh) helped with the administration and lab work. DSK is grateful to Anu Kaakinen (University of Helsinki) for supporting his trip to Iran, to Ursula Göhlich (NHMW) for crucial information on key specimens and providing photographs of Maragheh specimens, and to Zhang Zhaoqun (IVPP) for sharing information about the age of some Chinese sites. We also thank Alexandros Xafis (University of Vienna) for providing the photographic material of the Maragheh collection in NHMW. We appreciate comments by Denis Geraads and an anonymous reviewer that substantially improved our article. Raymond Bernor (Howard University, Washington DC) kindly polished the English of our text. This research did not receive any specific grant from funding agencies in the public, commercial, or not-for-profit sectors.

REFERENCES

- ATHANASSIOU A. 2014. — New giraffid (Artiodactyla) material from the Lower Pleistocene locality of Sesklo SE Thessaly, Greece): evidence for an extension of the genus *Palaeotragus* into the Pleistocene. *Zitteliana* B32: 71-89.
- BERNOR R. L. 1984. — A zoogeographic theater and biochronologic play: the time/biofacies phenomena of Eurasian and African Miocene mammal provinces. *Paléobiologie continentale* 14: 121-142.
- BERNOR R. L. 1986. — Mammalian biostratigraphy, geochronology, and zoogeographic relationships of the late Miocene Maragheh fauna, Iran. *Journal of Vertebrate Paleontology* 6: 76-95. <https://doi.org/10.1080/02724634.1986.10011600>
- BERNOR R. L., SEMPREGON G. & DAMUTH J. 2014. — Maragheh Ungulate Mesowear: Interpreting Paleodiet and Paleoecology from a Diverse Fauna with Restricted Sample Sizes. *Annales Zoologici Fennici* 51: 201-208. <https://doi.org/10.5735/086.051.0220>
- BOHLIN B. 1926. — Die Familie Giraffidae. *Paleaeontologia Sinica* C1: 1-178.
- BONIS L. DE, BRUNET M., HEINTZ E. & SEN S. 1992. — La province greco-irano-afghane et la repartition des faunes mammaliennes au Miocène supérieur. *Paleontologia i Evolució* 24-25: 103-112.
- CAMPBELL B. G., AMINI M. H., BERNOR R. L., DICKENSON W., DRAKE W., MORRIS R., VAN COUVERING J. A. & VAN COUVERING J. A. H. 1980. — Maragheh: A classical late Miocene

- vertebrate locality in northwestern Iran. *Nature* 287: 837-841. <https://doi.org/10.1038/287837a0>
- DANOWITZ M., HOU S., MIHLBACHLER M., HASTINGS V. & SOLOUNIAS N. 2016. — A combined-mesowear analysis of late Miocene giraffids from North Chinese and Greek localities of the Pikermian Biome. *Palaeogeography, Palaeoclimatology, Palaeoecology* 449: 194-204. <https://doi.org/10.1016/j.palaeo.2016.02.026>
- DENG T., QIU Z. X., WANG B. Y., WANG X. & HOU S. K. 2013. — Late Cenozoic Biostratigraphy of the Linxia Basin, northeastern China, in Wang X., Flynn L. J. & Fortelius M. (eds), *Fossil Mammals of Asia*. Columbia University Press, New York: 243-273. <https://doi.org/10.7312/wang15012>
- DEVYATKIN E. V. 1981. — The Cenozoic of Inner Asia. Trud. Sov. Mongol. Trudy Sovmestnaya Sovetsko-Mongolskaya Nauchno-Issledovatel'skaya Geologicheskaya Ekspeditsiya 27: 1-180.
- DMITRIEVA E. L. & NESMEJANOV S. A. 1982. — Mammals and stratigraphy of Tertiary continental deposits in South-Eastern Central Asia, Catalog of local. Trudy Paleontologicheskogo Instituta Akademii Nauk SSSR 193: 87-113.
- ERDBRINK D. P. B. 1976a. — A fossil Giraffine from the Maragheh region in NW. Iran. *Mitteilungen der Bayerischen Staatssammlung für Paläontologie und Histor. Geologie*. 16: 29-40.
- ERDBRINK D. P. B. 1976b. — Early *Samotherium* and early *Oioceros* from an Uppermost Vindobonian fossiliferous pocket at Mordaq near Maragheh in NW. Iran. *Mitteilungen der Bayerischen Staatssammlung für Paläontologie und Histor. Geologie*. 16: 41-52.
- ERDBRINK D. P. B. 1977. — On the distribution in time and space of three Giraffid genera with Turolian representatives at Maragheh in NW. Iran. *Proceedings Koninklijke Nederlandse Akademie van Wetenschappen B* 80: 337-355.
- ERDBRINK D. P. B. 1978. — Fossil Giraffidae from the Maragheh area, NW. Iran. *Mitteilungen der Bayerischen Staatssammlung für Paläontologie und Histor. Geologie*. 18: 93-115.
- ERONEN J. T., MIRZAEI ATAABADI M., MICHEELS A. KARME A. R. L. BERNOR R. L. & FORTELIUS M. 2009. — Distribution history and climatic controls of the Late Miocene Pikermian chronofauna. *Proceedings of the National Academy of Sciences* 106: 11867-11871. <https://doi.org/10.1073/pnas.0902598106> <https://doi.org/10.1073/pnas.0902598106>
- FORSYTH-MAJOR C. J. 1888. — Sur un gisement d'ossements fossiles dans l'île de Samos, contemporain de l'âge de Pikermi. *Comptes Rendus de l'Académie des sciences* 107: 1178-1182.
- GENTRY A. W., RÖSSNER G. E. & HEIZMANN P. J. 1999. — Suborder Ruminantia, in RÖSSNER G. & HEISSIG K. (eds), *The Miocene Land Mammals of Europe*. Verlag Dr. Friedrich Pfeil, Munich: 225-258.
- GERAADS D. 1978. — Les Palaeotraginae (Giraffidae, Mammalia) du Miocène supérieur de la région de Thessalonique (Grèce). *Géologie Méditerranéenne* 5: 269-276.
- GERAADS D. 1986. — Remarques sur la systématique et la phylogénie des Giraffidae (Artiodactyla, Mammalia). *Geobios* 19: 465-477. [https://doi.org/10.1016/S0016-6995\(86\)80004-3](https://doi.org/10.1016/S0016-6995(86)80004-3)
- GERAADS D. 1994. — Les gisements de mammifères du Miocène supérieur de Kemiklitepe, Turquie: 8. Giraffidae. *Bulletin du Muséum national d'histoire naturelle* 4^e sér. C 16: 159-173.
- GERAADS D. 2017. — Late Miocene large mammals from Mahmutgazi, Denizli province, western Turkey. *Neues Jahrbuch für Geologie und Paläontologie* 284 (3): 241-257. <https://doi.org/10.1127/njgpa/2017/0661>
- GODINA A. YA. 2002. — On the taxonomy and evolution of *Samotherium* (Giraffidae, Artiodactyla). *Paleontological Journal* 36: 395-402.
- GRAY J. E. 1821. — On the natural arrangement of vertebrate animals. *London medical repository* 15: 296-310.
- GREWINGK C. 1881. — Ueber fossile Säugethiere von Maragha in Persien. *Verhandlungen der K.K. Geologischen Reichsanstalt*, 296 p.
- GUNTHER R. T. 1896. — The Pliocene mammalia of the bone beds of Maragha. *Journal of the Linnean Society of London* 27: 376-378.
- HAILE-SELASSIE Y. 2009. — Giraffidae, in HAILE SELASSIE Y. & WOLDE GABRIEL G. (eds), *Ardipithecus kadabba; Late Miocene Evidence from the Middle Awash, Ethiopia*. University of California Press, Los Angeles: 389-395.
- HAMILTON W. R. 1978. — Fossil giraffes from the Miocene of Africa and a revision of the phylogeny of Giraffoidea. *Philosophical Transactions of the Royal Society B* 283: 165-229. <https://doi.org/10.1098/rstb.1978.0019>
- HOU S., CYDYLO M., DANOWITZ M. & SOLOUNIAS N. 2019. — Comparisons of *Schansitherium tafeli* with *Samotherium boissieri* (Giraffidae, Mammalia) from the late Miocene of Gansu Province, China. *PLoS ONE* 14: e0211797. <https://doi.org/10.1371/journal.pone.0211797>
- HOU S., DANOWITZ M., SAMMIS J. & SOLOUNIAS N. 2014. — Dead ossicones, and other characters describing Palaeotraginae (Giraffidae; Mammalia) based on new material from Gansu, Central China. *Zitteliana* 32: 91-98.
- INTERNATIONAL CODE OF ZOOLOGICAL NOMENCLATURE, 4th Ed., International Trust for Zoological Nomenclature, London, 1999.
- KAMEI T., IKEDA J., ISHIDA H., ISHIDA S., ONISHI L., PARTODIZAR H., SASAJIMA S. & NISHIMURA S. 1977. — A general report of the geological and paleontological survey in Maragheh area, North-West Iran. *Memoirs of the Faculty of Science, Kyoto University. Series of geology and mineralogy* 43: 131-164. <http://hdl.handle.net/2433/186612>
- KAYA F., BIBI F., ŽLIOBAIT I., ERONEN J. T., HUI T. & FORTELIUS M. 2018. — The rise and fall of the Old-World savannah fauna and the origins of the African savannah biome. *Nature Ecology & Evolution* 2: 241-246. <https://doi.org/10.1038/s41559-017-0414-1>
- KITTL E. 1885. — Die fossile Säugethier-fauna von Maragha in Persien. *Verhandlungen der K.K. Geologischen Reichsanstalt*: 397-399.
- KORDIKOVA E. G. 1998. — Main stages in the development of Mammalian faunas in the Oligocene and Miocene of Kazakhstan. *Vestnik Kaz GU, Seriya Biologicheskaya* 5: 165-180.
- KOSTOPOULOS D. S. 2009a. — The Pikermian Event: temporal and spatial resolution of the Turolian large mammal fauna in SE Europe. *Palaeogeography, Palaeoclimatology, Palaeoecology* 274: 82-95.
- KOSTOPOULOS D. S. 2009b. — The late Miocene mammal faunas of the Mytilinii Basin, Samos Island, Greece: New collection: 13. Giraffidae, in KOUFOS G. D. & NAGEL D. (eds), *The late Miocene mammal faunas of Samos. Beiträge zur Paläontologie* 31, Vienna: 299-343.
- KOSTOPOULOS D. S., KOLIADIMOU K. K., KOUFOS G. 1996. — The giraffids (Mammalia, Artiodactyla) from the late Miocene mammalian localities of Nikiti (Macedonia, Greece). *Palaeontographica Abtheilung* 239: 61-88.
- KOSTOPOULOS D. S. & SARAÇ G. 2005. — Giraffidae (Mammalia, Artiodactyla) from the late Miocene of Akkaşdağı, Turkey, in Sen S. (ed.), *Geology, mammals and environments at Akkaşdağı, late Miocene of Central Anatolia. Geodiversitas* 27: 735-745.
- KOUFOS G. D. 2013. — Neogene mammal biostratigraphy and chronology of Greece, in WANG X., FLYNN L. J. & FORTELIUS M. (eds), *Fossil Mammals of Asia*. Columbia University Press, New York: 595-621. <https://doi.org/10.7312/wang15012>
- LINNAEUS C. 1758. — *Systema naturae*, 10th edition, Vol. 1. Laurentii Salvii, Holmiae (Stockholm), ii, 824 p.
- MARRA A. C., SOLOUNIAS N., CARONE G., ROOK L. 2011. — Palaeogeographic significance of the giraffid remains (Mammalia, Artiodactyla) from Cessaniti (Late Miocene, southern Italy). *Geobios* 44: 189-197. <https://doi.org/10.1016/j.geobios.2010.11.005>
- MECQUENEM R. DE. 1924-1925. — Contribution à l'étude des fossiles de Maragha. *Annales de Paleontologie* 13/14: 135-160.
- MERCERON G., COLYN M. & GERAADS D. 2018. — Browsing and non-browsing extant and extinct giraffids: Evidence from dental microwear textural analysis. *Palaeogeography, Palaeoclimatology, Palaeoecology* 505: 128-139. <https://doi.org/10.1016/j.palaeo.2018.05.036>

- MIRZAEI ATAABADI M. 2010. — *The Miocene of western Asia; fossil mammals at the crossroads of faunal provinces and climate regimes*. PhD Thesis, Helsinki University print, Helsinki, 69 p.
- MIRZAEI ATAABADI M., BERNOR R. L., KOSTOPOULOS D., WOLF D., ORAK Z., ZAREE G., NAKAYA H., WATABE M., FORTELIUS M. 2013. — Recent Advances on Paleobiological Research of the Late Miocene Maragheh Fauna, Northwest Iran, in WANG X., FLYNN L. J. & FORTELIUS M. (eds), *Fossil Mammals of Asia*. Columbia University Press, New York: 544-563. <https://doi.org/10.7312/wang15012>
- MIRZAEI ATAABADI M., KAAKINEN A., KUNIMATSU Y., NAKAYA H., ORAK Z., PAKNIA M., SAKAI T., SALMINEN J., SAWADA Y., SEN S., SUWA G., WATABE M., ZAREE G., ZHANG Z., FORTELIUS M. 2016. — The late Miocene hominoid-bearing site in the Maragheh Formation, Northwest Iran. *Palaeobiodiversity and Palaeoenvironments* 96: 349-371. <https://doi.org/10.1007/s12549-016-0241-4>
- OWEN R. 1848. — Description of teeth and portions of jaws of two extinct Anthracotherioid quadrupeds (*Hyopotamus vectianus* and *Hyop. bovinus*) discovered by the Marchioness of Hastings in the Eocene depositon the NW coast of the Isle of Wight: with an attempt to develop Cuvier's idea of the Classification of Pachyderms by the number of their toes. *Quarterly Journal of the Geological Society* 4: 103-141.
- PARIZAD E., MIRZAEI ATAABADI M., MASHKOUR M. & SOLOUNIAS N. 2019. — First giraffid skulls (*Bohlinia attica*) from the late Miocene Maragheh fauna, Northwest Iran. *Geobios* 53: 23-34.
- QIU Z.-X., QIU Z.-D., DENG T., LI C.-K., ZHANG Z.-Q., WANG B. Y. & WANG X. 2013. — Neogene Land Mammal Stages/Ages of China. Toward the goal to establish an Asian Land Mammal Stage/Age scheme, in WANG X., FLYNN L. J. & FORTELIUS M. (eds), *Fossil Mammals of Asia*. Columbia University Press, New York: 29-90. <https://doi.org/10.7312/wang15012>
- RÍOS M., SÁNCHEZ I. M., & MORALES J. 2017. — A new giraffid (Mammalia, Ruminantia, Pecora) from the late Miocene of Spain, and the evolution of the sivathere-samothere lineage. *PLoS ONE* 12: e0185378. <https://doi.org/10.1371/journal.pone.0185378>
- RODLER A. & WEITHOFER K. A. 1890. — Die Wiederkäufer der Fauna von Maragha. *Denkschriften der Kaiserlichen Akademie der Wissenschaften in Wien* 57: 753-772.
- SAKAI T., ZAREE G., SAWADA Y., MIRZAEI ATAABADI M. & FORTELIUS M. 2016. — Depositional environment reconstruction of the Maragheh Formation, East Azarbaijan, northwestern Iran. *Palaeobiodiversity and Palaeoenvironments* 96: 383-398. <https://doi.org/10.1007/s12549-016-0238-z>
- SALMINEN J., PAKNIA M., KAAKINEN A., MIRZAEI ATAABADI M., ZAREE G., ORAK Z., & FORTELIUS M. 2016. — Preliminary magnetostratigraphic results from the late Miocene Maragheh Formation, NW Iran. *Palaeobiodiversity and Palaeoenvironments* 96: 433-443. <https://doi.org/10.1007/s12549-016-0239-y>
- SCOPOLI G. A. 1777. — *Introductio ad historiam naturalem, sistens genera lapidum, planatarum, et animalium hactenus detecta, caracteribus essentialibus donata, in tribus divisa, subinde ad leges naturae*. Gerle, Prague, 506 p.
- SENYÜREK M. S. 1954. — A study of the remains of *Samotherium* found at Taskinpaça. *Revue de la Faculté des Langues, d'Histoire et de Géographie de l'Université d'Ankara* 12: 1-32.
- SOLOUNIAS N. 2007. — Family Giraffidae, in PROTHERO D. R. & FOSS S. E. (eds), *The Evolution of Artiodactyls*. Johns Hopkins University Press, Baltimore: 257-277.
- SOLOUNIAS N. & DANOWITZ M. 2016. — The Giraffidae of Maragheh and the identification of a new species of *Honanotherium*. *Palaeobiodiversity and Palaeoenvironments* 96: 489-506. <https://doi.org/10.1007/s12549-016-0230-7>
- SOLOUNIAS N., MCGRAW W. S., HAYEK L.-A. C. & WERDELIN L. 2000. — The Paleodiets of the Giraffidae, in VRBA E. S. & SCHALLER G. B. (eds), *Antelopes, Deer and Relatives*. Yale University Press, New Haven: 84-95.
- SOLOUNIAS N., PLAVCAN J. M., QUADE J. & WITMER L. 1999. — The Paleocology of the Pikermian biome and the Savanna myth, in AGUSTÍ J., ROOK L. & ANDREWS P. (eds), *The evolution of Neogene terrestrial ecosystems, in Europe*. Cambridge University Press, Cambridge: 436-453.
- SOLOUNIAS N., RIVALES F. & SEMPREBON G. 2010. — Dietary interpretation and paleocology of herbivores from Pikermi and Samos (late Miocene of Greece). *Paleobiology* 36: 113-136. <https://doi.org/10.1666/0094-8373-36.1.113>
- SOLOUNIAS N., SEMPREBON G., MIHLBACHLER M. C. & RIVALS F. 2013. — Paleodietary Comparisons of Ungulates between the Late Miocene of China, and Pikermi and Samos in Greece, in WANG X., FLYNN L. J. & FORTELIUS M. (eds), *Fossil Mammals of Asia*. Columbia University Press, New York: 676-692. <https://doi.org/10.7312/wang15012>
- SOTNIKOVA M. V., DODONOV A. E. & PEN'KOV A. V. 1997. — Upper Cenozoic bio-magnetic stratigraphy of Central Asian mammalian localities. *Palaeogeography, Palaeoclimatology, Palaeoecology* 133, 243-258. [https://doi.org/10.1016/S0031-0182\(97\)00078-3](https://doi.org/10.1016/S0031-0182(97)00078-3)
- THOMAS H., SEN S. & LIGABUE G. 1980. — La faune Miocène de la formation Agha Jari du Jebel Hamrin (Irak). *Proceedings Koninklijke Nederlandse Akademie van Wetenschappen B* 83: 269-287.
- TLEUBERDINA P. A. 1988. — Typical localities of *Hipparion* fauna in Kazakhstan and their biostratigraphic correlation. *Materialy po istorii fauny i flory Kazakhstana* 10: 38-69.
- VANGENGHEIM E. & TESAKOV A. 2013. — Late Miocene Mammal Localities of Eastern Europe and Western Asia, in WANG X., FLYNN L. J. & FORTELIUS M. (eds), *Fossil Mammals of Asia*. Columbia University Press, New York: 521-537. <https://doi.org/10.7312/wang15012>
- WANG X., LI Q., QIU Z., XIE, G., WANG B., QIU Z., TSENG Z., TAKEUCHI G. & DENG T. 2013. — Neogene Mammalian Biostratigraphy and Geochronology of the Tibetan Plateau, in WANG X., FLYNN L. J. & FORTELIUS M. (eds), *Fossil Mammals of Asia*. Columbia University Press. New York: 274-292. <https://doi.org/10.7312/wang15012>
- YAMADA E., HASUMI E., MIYAZATO N., AKAHOSHI M., WATABE M. & NAKAYA H. 2016. — Mesowear analyses of sympatric ungulates from the late Miocene Maragheh, Iran. *Palaeobiodivers. Palaeoenviron.* 96, 445-452.
- XAFIS A., MAYDA S., GRÍMSON F., NAGEL D., KAYA T. & HALAÇLAR K. 2019. — Fossil Giraffidae (Mammalia, Artiodactyla) from the early Turolian of Kavakdere (Central Anatolia, Turkey). *Comptes Rendus Palevol* 18 (6): 619-642. <https://doi.org/10.106/crpv.2019.04.010>
- ZHANG Z., KAAKINEN A., LIU L., LUNKKA J., SEN S., GOSE W., QIU Z., ZHENG S. & FORTELIUS M. 2013. — Mammalian Biochronology of the Late Miocene Bahe Formation, in WANG X., FLYNN L. J., FORTELIUS M. (eds), *Fossil Mammals of Asia*. Columbia University Press, New York: 187-202. <https://doi.org/10.7312/wang15012>

Submitted on 30 July 2019;
accepted on 29 November 2019;
published on 1 December 2020.

APPENDICES — SUPPLEMENTARY MATERIAL.

APPENDIX 1. — Complementary description of dental and postcranial material. First *Samotherium* Major, 1888 (Giraffidae) skulls from the late Miocene Maragheh fauna (Iran) and the validity of *Alcicephalus* Rodler & Weithofer, 1890.

MATERIAL AND METHODS

Mandibular and dental measurements, and teeth nomenclature follow Kostopoulos *et al.* (1996 and literature therein), and Kostopoulos (2009b, 2016). Astragalar and metapodial morphology follow Rios *et al.* (2016), and Solounias & Danowitz (2016). All the measurements are in millimeters.

SYSTEMATIC PALEONTOLOGY

Class MAMMALIA Linnaeus, 1758
Order ARTIODACTYLA Owen, 1848
Suborder RUMINANTIA Scopoli, 1777
Family GIRAFFIDAE Gray, 1821
Genus *Samotherium* Forsyth-Major, 1888

Samotherium cf. *boissieri*
(Appendices 2-5)

REFERRED MATERIALS. — Upper tooththrows of cranial specimens PRCI/M350, PRCI/M351, and four mandibles (PRCI/M310-313)

PROVISIONALLY ASCRIBED. — Two metapodials (PRCI/M174, 312), and six astragali (PRCI/M294, 296-300).

SITE. — Ruhanioon locality, Maragheh, Iran.

DESCRIPTIONS

Upper dentition

The P2-M3 length ranges between 183 mm (PRCI/M350) and 185 mm (PRCI/M351) (Table 1), with a premolar/molar ratio of 65.6 and 69.0, respectively. P2 and P3 are linguall rounded without evidence of a protocone-hypocone distinction. P3 compared to P2 has a stronger parastyle and a weaker metastyle, but none of them shows distinction of paracone from metacone. A hypoconal fold (spur) is present on both the P2 and P3. P4 is similar to P3, but much wider with strong parastyle and metastyle (Figs 2F; 3D). It has an almost flat and oblique lingual wall.

The molars, especially M2 and M3, are characterized by strong styles and paracone pillar. Well developed buccal and thin lingual cingula, and weak basal pillars attached to the distal lobe are present (Figs 2F; 3D). The protocone is more projected linguall than the hypocone, but none of them appears linguall constricted. On the less worn specimen (PRCI/M351) the mesial flange of the hypocone of M2 and M3 shows a small spur. It contacts the distal flange of the protocone, whereas the labial end of the mesial hypoconal flange contacts the distolingual part of the paracone. The enamel is finely rippled.

Mandibles and lower dentition

The preserved mandibles represent individuals ranging in age from young adult to old. The studied material includes: two right

mandibular rami with p2-m3 (PRCI/M312, Appendix 4B; PRCI/M311, Appendix 4D), and two left mandibular rami with p2-m3 (PRCI/M310, Appendix 4C; PRCI/M313, Appendix 4A). The mental foramen is visible in some of the specimens. It opens about 50 mm in front of p2, suggesting the diastema is shorter than the cheek teeth row (Appendix 2). The horizontal ramus has a concave ventral profile between the mental foramen and the p2 (Appendix 4A1, A2, B1, B2, C1, C2, D1, D2). The mandibles have a generally wide angle, which slightly projects postero-ventrally. The vertical part of the ramus is not preserved, but in PRCI/M313-312 (Appendix 4A, B), the anterior margin of the ascending ramus behind the m3 forms a 60-70° angle with the alveolar level. The pterygoid and the masseteric fossae are shallow and slightly marked in some specimens. The p2-m3 length ranges between 189-190 mm (Appendix 2). The lower premolar/molar ratio ranges from 58 to 63 (mean = 60.5, n = 4).

The p2 is simple and long, representing 80-90% of the p3 length. An antero-lingual styloid is well developed and distinct. The entoconid, entostyloid, hypoconid, and parastyloid are well-developed on p2. The metaconid is present and centrally placed. It is rounded, and independent. The paraconid is absent. The p3 is molarized though the metaconid and the paraconid remain independent till advanced wear stage (Appendix 4A (3), B (3), C (3)). Buccally, the hypoconid is clearly distinct from the protoconid but not much projected. The parastyloid is strong. The entoconid is obliquely placed. The p4 looks like a large version of p3 but the paraconid and the metaconid are fully merged (Appendix 4A3, B3, C3). Connection of the postmetacristid and entoconid is visible with wear. Both the p3 and p4 show a reduced talonid compared to the trigonid (Appendix 4A3, B3, C3).

The molars are simple, moderately wide, with well-marked paraconid and weak parastyloid and metastyloid (Appendix 4A3, B3, C3). The longer anterior and wider posterior lobes are well developed and separated by a deep labial notch. The third lobe of m3 is round to elliptical shaped in occlusal view, single cuspid and arranged along the longitudinal axis of the tooth.

Postcranials

A few postcranials from Ruhanioon locality are provisionally associated with the cranial material described above (Appendix 5). The material includes a metacarpal (PRCI/M174, Appendix 5D-F), a metatarsal (PRCI/M312, Appendix 5A-C), and six astragali (PRCI/M294, 296-300, Appendix 5G-R). Measurements are provided in Appendix 3. The medial and lateral epicondyles (*sensu* Rios *et al.* 2016: fig. 1) of Maragheh metacarpal are subequal but asymmetrical. There is a groove in the center of the medial epicondyle, while the lateral one has an oblique groove. The metatarsals also possess asymmetrical proximal epicondyles. The medial epicondyle is broad and a groove split it into two surfaces. It is shorter

than the lateral epicondyle, which is confined and rounded. An oval-shaped body, which protrudes proximally, is wedged between epicondyles. A central trough with medium depth is present on the shaft of metapodials, defined by a rounded medial ridge, and a sharp lateral one. The keels of the distal condyles also extend into the distal shaft.

The trochlea of the astragalus shows a higher and thicker lateral proximal edge than the medial one. The central fossa is large, as high as wide. The distal intracephalic fossa is large and rather deep laterally. The medial surface of the collum tali bears a prominent crest. The medial side of the distal astragalar head is more massive than the lateral one. The trochlea distinguishes laterally from the head by a clear notch.

POSTCRANIAL COMPARISON AND DISCUSSION

By their absolute size, the studied metapodials and astragali are clearly smaller than those of *Samotherium major* from Samos and smaller than postcranials ascribed to *S. neumayri* from Maragheh (based on postcranial collection in MNHN, Paris) (Appendix 6). They fall well within the range of variation of *Samotherium boissieri* Major, 1888 from Samos and *Palaeotragus coelophrys* Rodler & Weithofer, 1890 from Maragheh (based on postcranial collection in MNHN, Paris) (Appendix 6). Postcranial distinction between the two latter palaeotragine taxa is, however, much more delicate and proportionally infeasible. As the presence of *Palaeotragus coelophrys* in Ruhanioun locality is more than expected, though not yet confirmed by cranial or dental material, we focus our comparison on some morphological features that may serve discriminating postcranials of these two taxa.

In both the metacarpal and the metatarsal from Ruhanioun locality in Maragheh, the passage from the distal diaphysis to distal epiphysis is rather abrupt forming a clear “neck” feature that gives to the distal epiphysis a more rectangular shape in both anterior and posterior views. Though variability exists,

metapodials of *S. boissieri* in NHMUK show the same pattern. Metapodials of *Palaeotragus rouenii* Gaudry, 1861 and large-sized *Palaeotragus* ascribed to *P. ex. gr. coelophrys* (including two specimens in MNHN, Paris collection and the specimen NHMUK M4711 from Maragheh identified as *P. coelophrys*) show a more evenly transition from the distal diaphysis to the distal epiphysis and thus a more triangular outline.

As in *S. boissieri*, most of the studied astragali show a strong distal intracephalic fossa, oblique medial ridge, and a clear lateral notch on the lateral dorsal edge. A sharp medial scala and a well-marked angle between the lateral ridge of the trochlea and the lateral distal head of the astragalus also exist. The specimen PRCI /M297 (Appendix 5K, Q) is the one in which most of these features are not apparent. In a restricted but indicative sample of large-sized *Palaeotragus* astragali from several institutions (including a few Maragheh specimens), the lateral edge of the dorsal surface is fairly straight and the notch much less expressed. The distal intracephalic fossa is weak, and the medial ridge runs along the very medial edge of the ventral side. The medial scala is weaker. Although most of the above mentioned postcranial differences have to be cross-checked based on a large sample, they indicate that the majority of the studied postcranials better match *S. boissieri* than *P. coelophrys*.

ADDITIONAL REFERENCES

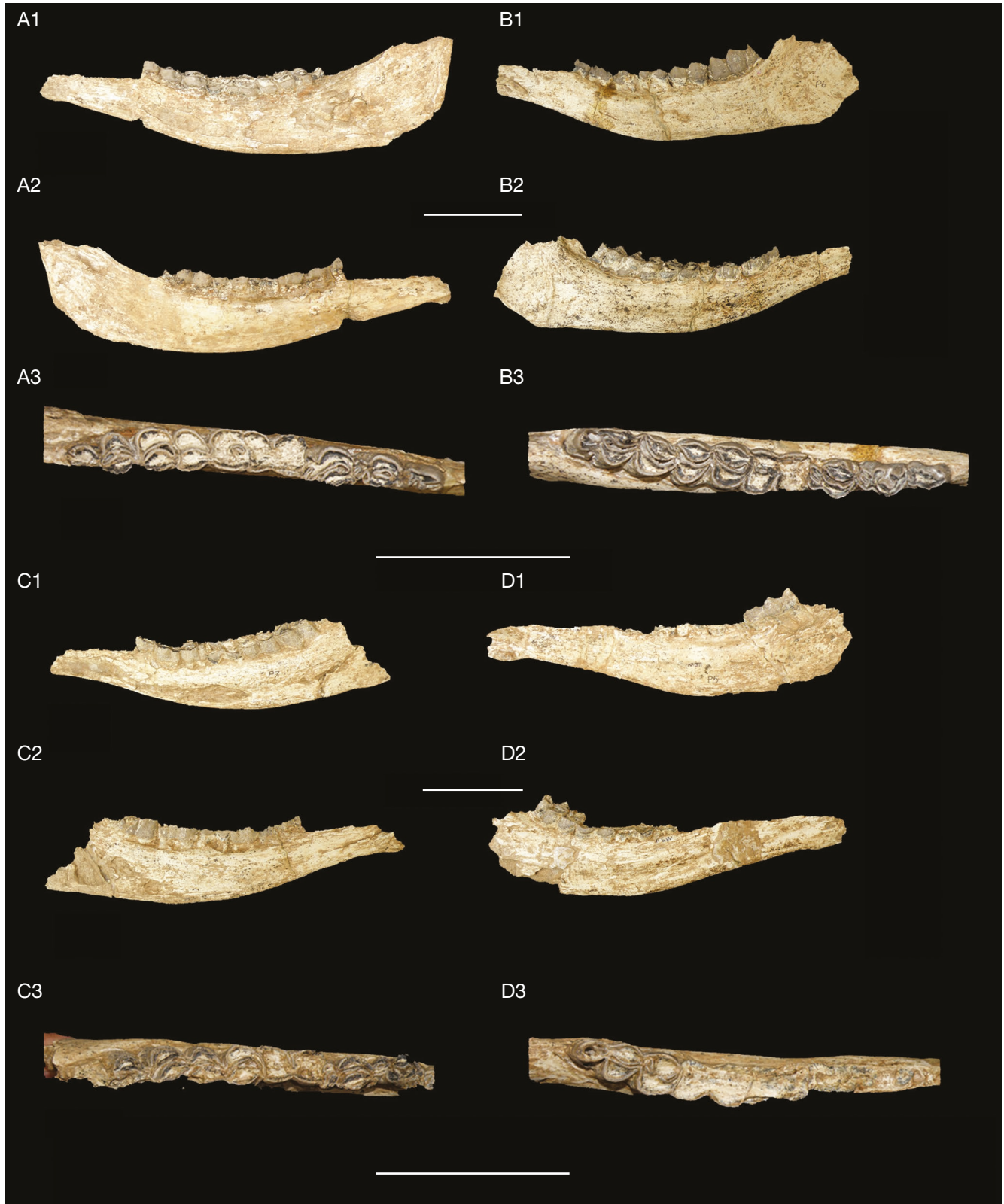
- KOSTOPOULOS D. 2016. — Artiodactyla, in KOUFOS G. D. & KOSTOPOULOS D. S. (eds), *Palaeontology of the upper Miocene vertebrate localities of Nikiti (Chalkidiki Peninsula, Macedonia, Greece)*. Geobios 49, Lyon: 119-134.
- RIOS M., DANOWITZ, M. & SOLOUNIAS N. 2016. — First comprehensive morphological analysis on the metapodials of Giraffidae. *Palaeontologia Electronica* 19.3.52A: 1-39.
- SOLOUNIAS N. & DANOWITZ M. 2016. — Astragalar Morphology of Selected Giraffidae. *PLoS ONE* 11 (3): e0151310. <https://doi.org/10.1371/journal.pone.0151310>

APPENDIX 2. — Measurements (in mm) of *Samotherium* cf. *boissieri* Major, 1888 mandibles from the Maragheh Formation, NW Iran. **Bold numbers** refer to measurements, (c.) indicates approximately. Measurements: **1**, length from the angle: Gonion caudal-Infradentale; **2**, length of the diastema: oral border of the alveolus of p2- mental foramen; **3**, length from the most aboral point of the alveolus behind m3- mental foramen; **4**, length of the tooth row (p2-m3), measured along the alveoli on the buccal side; **5**, length of the premolar row (p2-p4), measured along the alveoli on the buccal side; **6**, length of the molar row (m1-m3), measured along the alveoli on the buccal side; **7**, height of the mandible behind m3 from the most aboral point of the alveolus on the buccal side; **8**, height of the mandible in front of p2; **9**, ventral width of the mandibular corpus in front of p2; **10**, ventral width of the mandibular corpus behind m3; **11**, transverse (mediolateral) diameter of the mandibular condyle; **12**, Length of p2; **13**, Width of p2; **14**, Length of p3; **15**, Width of p3; **16**, Length of p4; **17**, Width of p4; **18**, Length of m1; **19**, Width of m1; **20**, Length of m2; **21**, Width of m2; **22**, Length of m3, **23**, Width of m3.

Specimen	1	2	3	4	5	6	7	8	9	10	11	12
M310		c. 84.7	275	189	71.2	118.8	73.1	45.5	17.7	18.2		21
M311		97.7	300	190	73.5	116.3	c. 84.7	49.7	20.4	27.6		
M312			190	69.4	115.3	77.7	46	21.1	20.9	20.9	c.110	19
M313	425	c.103	298	190	69.5	118.5	81.4	46.5	18.9	22.4	c.125	17.5
	13	14	15	16	17	18	19	20	21	22	23	
M310	11.2	23.7	15.9	23.7	18.3	37	23.5	41.5	23.1	55.3	20.4	
M311		25.6	16.6			32.5	22.5	40	24.6	54	25.4	
M312	11.6	25	15.5	25	19	34.7	25.5	42	24.7	49.5	21.2	
M313	9.5	23.8	16	25.1	20.4	31.9	23.2	41	24.3	55.3	23.1	

APPENDIX 3. — Measurements (in mm) of provisionally *Samotherium* cf. *boissieri* Major, 1888 postcranials from the Maragheh Formation, NW Iran. **Bold numbers** refer to measurements. M312 (Mt), M174 (Mc), M294-300 (Ast). Measurements: **1**, total length; **2**, transverse diameter of the proximal end; **3**, antero-posterior diameter of the proximal end; **4**, transverse diameter of the diaphysis; **5**, antero-posterior diameter of the diaphysis; **6**, transverse diameter of the distal end; **7**, antero-posterior diameter of the distal end; **8**, lateral length of astragalus; **9**, medial length of astragalus; **10**, distal transverse diameter of the astragalus.

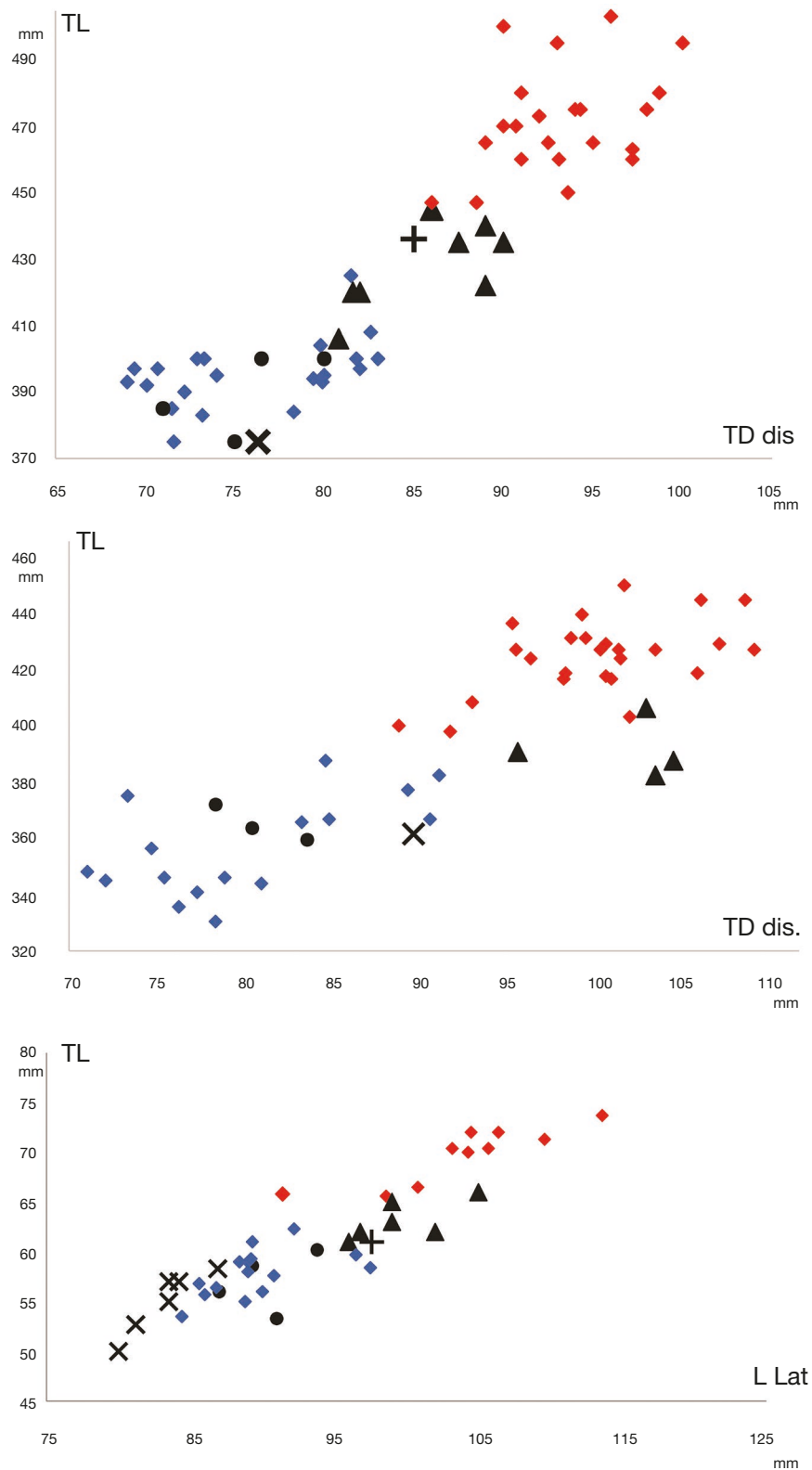
Specimen	1	2	3	4	5	6	7	8	9	10
M312	375	67.5	63.5	40.5	50.5	76.3	41.2			
M174	360	74.5	51.8	43.8	38.5	88.8	48.5			
M294								81.2	72	52.7
M296								83.5	74	55
M297								80	71.2	49.8
M298								84.2	75.2	57
M299								86.9	77.3	58.3
M300								83.5	73.6	57



APPENDIX 4. — *Samotherium cf. boissieri* Major, 1888 (PRCI/M310-313) mandibles from Ruhanioun locality, Maragheh, NW Iran. M313: **A1**, labial; **A2**, lingual; and **A3**, occlusal views. M312: **B1**, lingual; **B2**, labial; **B3**, occlusal views. M310: **C1**, labial; **C2**, lingual; **C3**, occlusal views. M311: **D1**, lingual; **D2**, labial; and **D3**, occlusal views. Scale bars: 10 cm.



APPENDIX 5. — *Samotherium* cf. *boissieri* Major, 1888 (PRCI/M174, 294, 296-300, 312) postcranials from Ruhanioun locality, Maragheh, NW Iran. **A**, Posterior; **B**, lateral; and **C**, anterior view of metatarsus M312. **D**, Anterior; **E**, lateral; and **F**, posterior view of metacarpus M174. Dorsal views of astragali: **G**, M299; **H**, M298; **I**, M296; **J**, M294; **K**, M297; and **L**, M300. And plantar views of astragali: **M**, M299; **N**, M298; **O**, M296; **P**, M294; **Q**, M297; and **R**, M300. Scale bars: 10 cm.



APPENDIX 6. — Scatter diagram comparing: **A**, the metatarsal; **B**, the metacarpal; and **C**, astragali proportions of *Samotherium* cf. *boissieri* Major, 1888 (×) and *S. neumayri* Rodler & Weithofer, 1890 (▲) from Maragheh, Iran with *S. boissieri* (blue ♦) and *S. major* Bohlin, 1926 (red ♦) from Samos, Greece, and *Palaeotragus coelophrys* Rodler & Weithofer, 1890 (●) from MNHN collection. Horizontal and the vertical axis represent measurements in millimeters. Abbreviations: **TL**, total length; **TD dis.**, distal transverse diameter; **L lat**, lateral length. Maragheh specimens (×); Mt: PRCI/M312 in **A**; Mc: PRCI/M174 in **B**; Ast: M294-300 in **C**; and (+) MNHN MAR 571 in **A**; MNHN MAR 838 in **C**. Samos data after Kostopoulos (2009b).